ETH Zurich

QUANTUM DEVICE LAB

Semester project

Surface Acoustic Wave Resonators

Denis LOOS

Supervisor: Dr. Pasquale SCARLINO
Principal Investigator: Prof. Dr. Andreas WALLRAFF

December 18, 2017

Abstract

This work concerns the optimization of surface acoustic wave (SAW) resonators built on GaAs substrates. Surface Acoustic Waves (SAW) are produced on a piezoelectric substrate by applying an oscillating potential through an interdigital transducer (IDT). An IDT consists of a series of metallic lines: when an oscillating potential is applied, each couple of consecutive lines behaves as a capacitor, producing an electric field that deforms the piezoelectric substrate.
The sound velocity can be slightly changed by the presence of a thin layer of metal on top of a piezoelectric material. Therefore a periodic structure of metallic fingers can be used in order to build a distributed Bragg reflector. Two of these mirrors in series make a cavity, where the confined SAW can interfere constructively. A SAW carries with it an electric field as it propagates. This field can be coupled with other physical systems, such as a transmon superconducting qubit or a double quantum dot semiconductor qubit. A preliminary study on GaAs was carried out in order to understand the best geometry suitable for high quality SAW cavities: a range of different mirror spacings, different number of electrodes in the Bragg reflectors and in the emitter, different electrode lengths as well as two different designs for the emitter were used. The best devices were selected for a systematic study of the Q-factors of resonators on GaAs.
SAW resonators in the GHz frequency range have been found to have low losses already at 4.2 K. The overall trends of the internal and external quality factor as a function of the SAW resonator parameters have been observed. This study opens up possibilities to make use of the phonon degree of freedom in future superconducting-semicondcutor hybrid devices.

Contents

1 Introduction

In recent years, the field of circuit-QED [5], researching the interaction between photons and solid-state qubits and their possible usage for quantum computing architectures, has been mostly using superconducting resonators to initialize, address and read out these systems. In this semester project, an alternative approach is presented, based on the usage of surface acoustic wave resonators [3]. By using the piezoelectric effect to convert the incoming electronic signal into surface phonons, these electromechanical resonators could be potentially used to address qubits and perform computations. This project represents a preliminary study of the quality factors of the surface acoustic wave (SAW) resonators as a function of different geometric parameters of these resonators, in order to optimize them and to couple them in the future with an artifical atom.

2 Theory of surface acoustic waver resonators

2.1 Surface acoustic waves

Surface waves exist in different variations, depending on the relative magnitude and phase of longitudinal and transversal components, as described for example in [6]. We will consider so called Rayleigh waves. These waves have a transversal and a longitudinal component that decay exponentially into the material. The two components have a relative phase difference which makes them form an elliptical curve at the top of the material, see Fig. 1. The major axis is usually orthogonal to the surface of the material and the sense of rotation is against the motion of the wave at the top of the ellipse. The velocity of these waves is usually of the order of km/s. To build a resonator for these

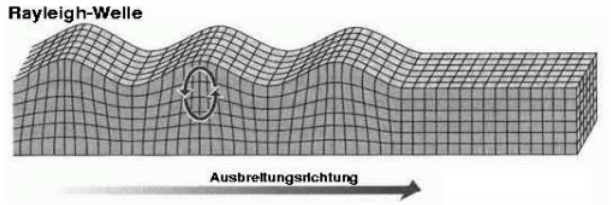

Figure 1: Rayleigh wave, *Kontinuumsmechanik* Lecture notes of Prof. Sigrist from spring semester 2016

waves, one needs a way to excite the waves and some kind of mirrors to create reflection and confine the waves.

2.2 Piezoelectric effect and inter-digital transducer

For the excitation of the surface acoustic waves, one takes advantage of the piezoelectric effect of the substrate, intrinsic GaAs in the case of this thesis. In order to increase

the conversion efficiency between electric power and mechanical power, it is necessary to minimize the presence of free carriers as any free carriers would couple to the electric field, drastically reducing the quality factors of the resonator.

An inter-digital transducer, IDT, consisting of an array of alternatively input and output or grounded fingers, converts the electrical signal into an acoustic signal and vice versa. This transducer is used to drive and detect the surface acoustic waves. Each finger generates a propagating wave and those then constructively interfere if the frequency of the input matches the condition $f_0 = \frac{v_{SAW}}{\lambda_0}$ where f_0 is the resonance frequency, λ_0 the wavelength and v_{SAW} the surface phonon propagation velocity. These surface phonons then propagate in both directions from the transducer. The fingers are created depositing a thin layer of aluminium on top of the GaAs using basic photolithography and then electron beam lithography at 100 keV. The advantage of Al is that it is very light (small mass loading effects) [1] and it becomes a superconductor at low temperatures.

The fingers of the transducer can have different designs. The easiest is an alternating pattern of signal and grounded fingers. The main problem with this is that it creates a lot of mechanical reflections [1]. These reflections severely reduce the amount of waves that can flow through the transducer and therefore leads to a decoupling of the two halves of the cavity, effectively creating two cavities coupled weakly by the transducer, as will be seen in section 4.1.1. A better approach is to use a double finger design. The advantage is that mechanical reflections are removed. The main problem with this design is that for the same wavelength, the features need to have half the size, i.e. one eighth of the wavelength instead of one fourth.

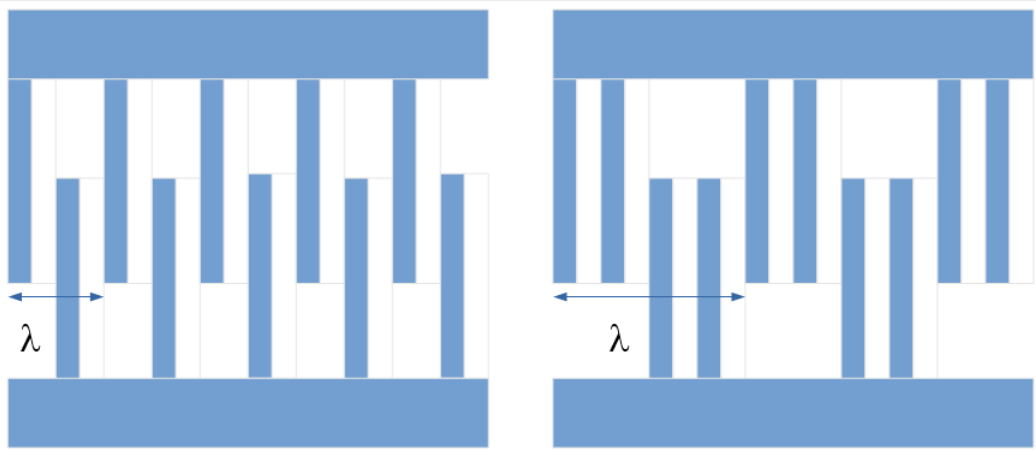

Figure 2: Single and double finger design

2.3 Reflectors

To reflect the surface acoustic waves and create a cavity, distributed Bragg reflectors (DBR), formed by large arrays of fingers, are fabricated on each side of the IDT. These

fingers induce very small changes in the propagation velocity of the waves underneath them and therefore generate a partial reflection [6]. The reflection coefficient of a single finger should conveniently be kept small [3]. Mirror fingers, that induce a larger change in the velocity of the waves would generate a lot of bulk waves propagating into the substrate, therefore dissipating energy. A large number of fingers with a reflectivity of a few percent is used in order to achieve a global reflection coefficient of the mirror close to 1. The spacing between two consecutive fingers of the DBR needs to be the wavelength of the waves created by the IDT to always create constructive interference. Furthermore, the spacing between the two mirrors needs to be an integer multiple of the wavelength, as in a typical Fabry-Perot interferometer.

The resonators can be built as 1-port or 2-port devices. With a 1-port device as in Fig. 3, one side of the IDT is receiving the input signal and also measuring the reflected signal and the other side is grounded. For 2-port devices as in Fig. 4, a second transducer is inserted into the cavity. This IDT is grounded on one side and the transmission is measured on the other contact of this second transducer. Both designs allow full characterization of the device, but single port devices are easier to measure as only a single connector is needed for each resonator. The position of the transducer within the cavity has to be carefully controlled. To give the best possible coupling of the transducer(s) to the cavity, the position of the metallic fingers need to match the position of the maxima of the modes supported by the cavity. In our devices, the IDT has been placed in the middle of the cavity, but shifting it about half a wavelength should give the same results.

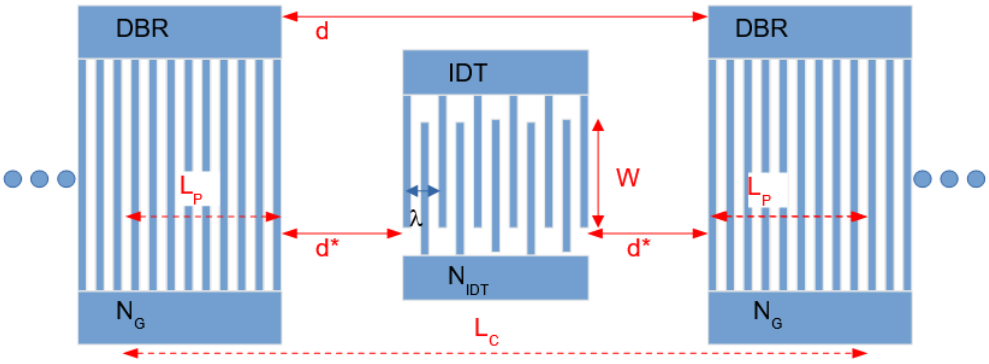

Figure 3: Schematic of a single-port SAW resonator

2.4 Internal and external losses

Ideally, internal losses are mainly dominated by the finite grating reflectivity, so by the impossibility of reflecting all of the incoming wave. Other contributions come from dissipation into bulk phonons, finite resistivity in the fingers, surface acoustic wave absorption in the substrate, mainly related to the presence of free carriers, and diffraction

N_{IDT}	Number of fingers in the IDT
N_G	Number of fingers in each grating
d	Mirror spacing
$L_p = \frac{\tanh((N_G-1)r_S)\lambda_0}{4r_s} \approx \frac{\lambda_0}{4\lvert r_S\rvert}$	Penetration depth into the reflector
	Approximation valid for typical values of N_G
$L_C = d + 2L_P$	Total cavity length
r_s	Reflectivity of one strip in the mirror
W	Finger length, width of the cavity
d^*	Spacing between the first finger of the mirror and the first finger of the IDT

Table 1: Definition of parameters

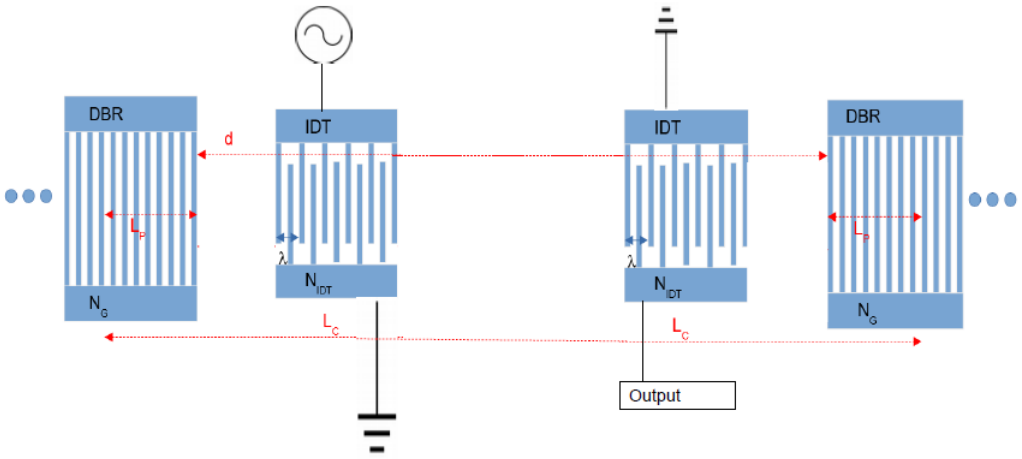

Figure 4: Double-port resonator design

[10]. The reflectivity of each finger contains two components [10]. The first part is a mass-loading part and the second part a piezoelectric part: $|r_S| = a + b\frac{h}{\lambda_0}$, where h is the thickness of the deposited fingers on the material and λ_0 the wavelength of the cavity. a and b are material constants. This functional form also means that the fingers of the grating are not allowed to be too thick otherwise the mass-loading will be important and severely reduce the quality factor by dissipating more energy into the substrate by bulk phonons.
The contribution to the internal quality factor, which comes from imperfect gratings, can be written as:

$$Q_0 = \frac{\pi(d + 2L_p)}{\lambda_0(1 - \tanh(|r_S|\, N_G))} \tag{1}$$

Another possible important contribution coming from diffraction following [10], has

$v_{SAW} = 2864$ m/s	Surface sound velocity in GaAs
$h = 25 - 30$ nm	Thickness of Al deposition
Z_c	Characterisitc impendance of the feed lines
$C_S = 1.2$ pF/cm	Effective dielectric constant
$K^2 = 0.07$	Piezoelectric coupling coefficient
$\gamma = -0.537$	Diffraction coefficient

Table 2: Material constants from [1]

the following form:

$$Q_{\text{Diffraction}} = \frac{5\pi}{|1+\gamma|}\left(\frac{W}{\lambda_0}\right)^2 \tag{2}$$

With the material parameters for GaAs from Table 2 and $W = 100\lambda_0$ for a typical cavity realized in this project, the internal quality factor from diffraction would be limited to $Q \propto 340000$ by diffraction. As quality factors add up reciprocally, we will see that this is not the limiting factor for the quality factors of our resonators.

As mentioned above, at every reflection some part of the waves dissipate into the material as bulk waves. This is largely dependent on the thickness of the deposited features, but is small for the usual fabrication parameters with $\frac{h}{\lambda_0} < 2\%$. Finally, losses also occur from the interaction with thermal phonons (negligible at cryostat temperatures) and defects and free carriers in the material.

The external quality factor is mainly determined by the geometry of the IDT and the SAW cavity as well as by the material and external circuit parameters. Single finger transducers create stronger couplings but have higher internal mechanical reflections. These can be reduced by using a double finger design. Following [10], with the definitions from table 2:

$$Q_{ext} = \frac{1}{5.74 v_{SAW} Z_C C_S W K^2 \left(0.5 N_{IDT}\right)^2} \cdot L_c \tag{3}$$

2.5 Peak separation

In a first approximation, the bandwidth of an IDT is $\frac{f_{IDT}}{N_{IDT}}$ [2]. The cavity also has a bandwidth, the free spectral range, coming from from basic resonator standing wave requirements, by considering the cavity as an acoustic Fabry-Perot. As usual, the mode frequencies must satisfy $L_C = n\lambda_0/2$ where L_C is the effective cavity length as defined in Fig. 3.

The Bragg reflectors generate a stop band. Only frequencies within this stop band will be visible in the spectrum. Following [10], the first stop band is $\Delta f = \frac{2 f_0 \left|r_S\right|}{\pi}$. So a larger stop band will allow for more resonances to be visible from the limitations imposed by the IDT and the cavity. When calculating these peak separations for some of the devices studied in the project, one can see that it comes mostly from the spacing of the mirrors. The bandwidth of the transducer, for the designs used in this project, is of the

Peak separation from IDT geometry	$\Delta f_{IDT} = \frac{f_0}{N_{IDT}}$
Peak separation from mirror spacing	$\Delta f_d = \frac{v_{SAW}}{2L_C}$
Stop band of the grating	$\Delta f_G = \frac{2f_0 \lvert r_S \rvert}{\pi}$

Table 3: Bandwidths expressed in frequency bands

order of 100 MHz, which is a lot larger than the first stop band of the mirrors. The bandwidth of the mirror spacing on the other hand produces separations of a few tens MHz which is what is also observed in the spectra of the devices.

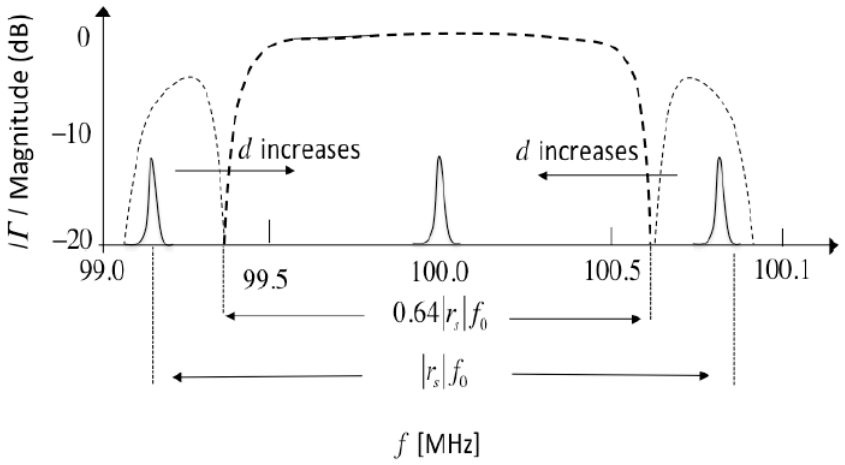

Figure 5: [10]: Illustration of the first stop band of the distributed Bragg reflectors (DBR) (dashed line). Only one resonance is within the band, but for increasing mirror spacing d (see Fig. 3), the free spectral range becomes smaller and the peaks move into the DBR stop band and will become visible.

2.6 Goal of the project and future coupling to an artificial atom

The main idea is to use surface acoustic wave resonators as a quantum bus connecting different qubits, as proposed in [4]. One of the possible implementations of a 2-level qubit system can be a charge qubit realised in GaAs as a 2 dimensional electron gas [7]. This kind of substrates is quite similar, in terms of piezoelectric properties to the bare GaAs used for our surface acoustic wave resonator optimization process. A double quantum dot is a system of 2 coupled islands with a tunnelling barrier between them [7]. This electric charge couples to the electric field created in the SAW cavity. In the usual rotating-wave approximation, the Hamiltonian of the coupled system takes the form of

a usual Jaynes-Cunnings Hamiltonian [3]:

$$H_{dot} = \delta S^z + g_{ch}\frac{2t_c}{\Omega}\left(S^+a + S^-a^+\right) \tag{4}$$

with δ the detuning between the cavity and the qubit, S the spin rising and lowering operators of the dot and a and a^+ the annihilation and creation operators for the phonon cavity. For the interaction strength, [3] estimates $g_{ch} = e\phi_0 F(kd)\sin(kl/2)$, with ϕ_0 the amplitude of the piezoelectric potential from a single phonon and the term $\sin(kl/2)$ describing the propagation of the mode between the two dots separated by a distance l. $k = \frac{2\pi}{\lambda_{SAW}}$ is the wavenumber of the surface acoustic wave. As plotted in Fig. 6, $F(kd)$ describes the decay of the surface acoustic wave into the bulk of the substrate, with d being the distance of the double quantum dot from the GaAs surface where the SAW will be generated.

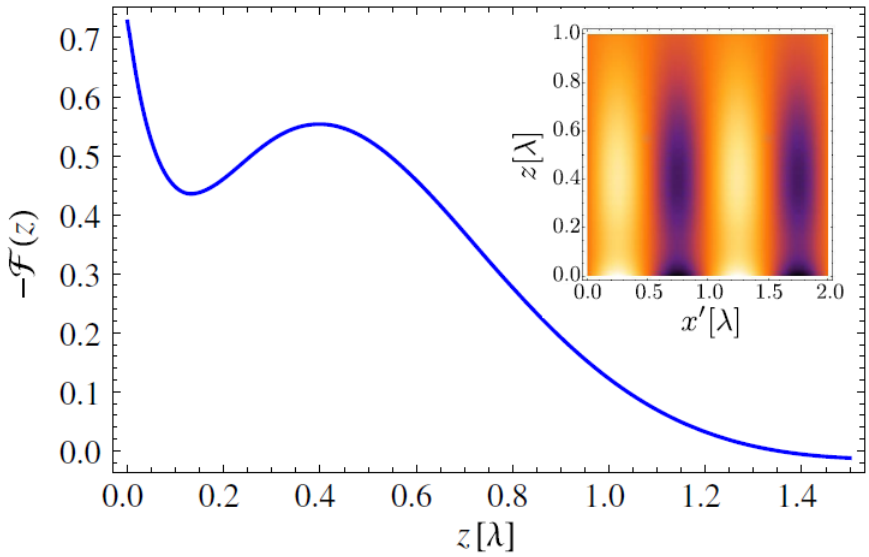

Figure 6: [10]: Plot of the function describing the decay of the surface acoustic wave into the bulk of the substrate along the direction z perpendicular to the surface expressed in λ. The inset shows the potential of the wave in the bulk.

The eigenstates of the quantum dot Hamiltonian $H = \frac{\epsilon}{2}\sigma^z + t_c\sigma^x$ are split by an energy $\Omega = \sqrt{\epsilon^2 + 4t_c^2}$. Usually, the double quantum dot parameters can be tuned such that $\Omega \sim$ few GHz, which is the same frequency regime that we are exploring with surface acoustic wave cavities.

To be able to efficiently read out the hybrid system, it is preferable to use an overcoupled resonator. In an overcoupled resonator, the internal losses are lower than the external coupling. Whereas this regime is typically easy to achieve in superconducting resonators, this is more difficult to reach in surface acoustic wave resonators on GaAs

for the geometries typically used in this thesis. In fact the external quality factor of a SAW cavity is usually larger by a factor of 10-100 than the internal quality factor. As seen from equations 1 to 3 in subsection 2.4, one way to increase the coupling would be to increase the cavity width W or the mirror spacing d. Both of these parameters lead to an increase of the cavity area A, which is directly linked to the acoustic coupling $g_{ch} \propto \frac{1}{\sqrt{A}}$ [3]. The derivation of this dependency comes from the zero-point mechanical motion of a phonon, which is directly proportional, through the piezo-electric effect, to the zero-point voltage fluctuations.

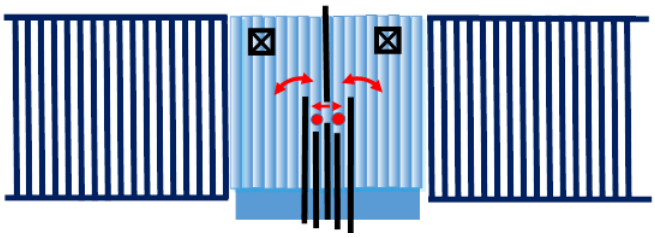

Figure 7: Schematic of the transducer and the underlying double quantum dot gate structure.

The main goal of the project is to produce a first analysis at 4K of the dependence of the quality factors of surface acoustic wave resonators on the different geometric factors in the design.

3 Experimental Setup

To characterize the surface acoustic wave resonators, a vector network analyser is used. The device allows to scan the excitation frequency over a certain frequency range and to observe the response of the cavity by measuring the S parameters of the system [9]. This allows to find the resonances of the SAW resonator, which then can be fitted to the theoretical models of the S parameters to extract the quality factors of the cavity. In this project, the design of the cavity consists of a single port surface acoustic wave resonator.

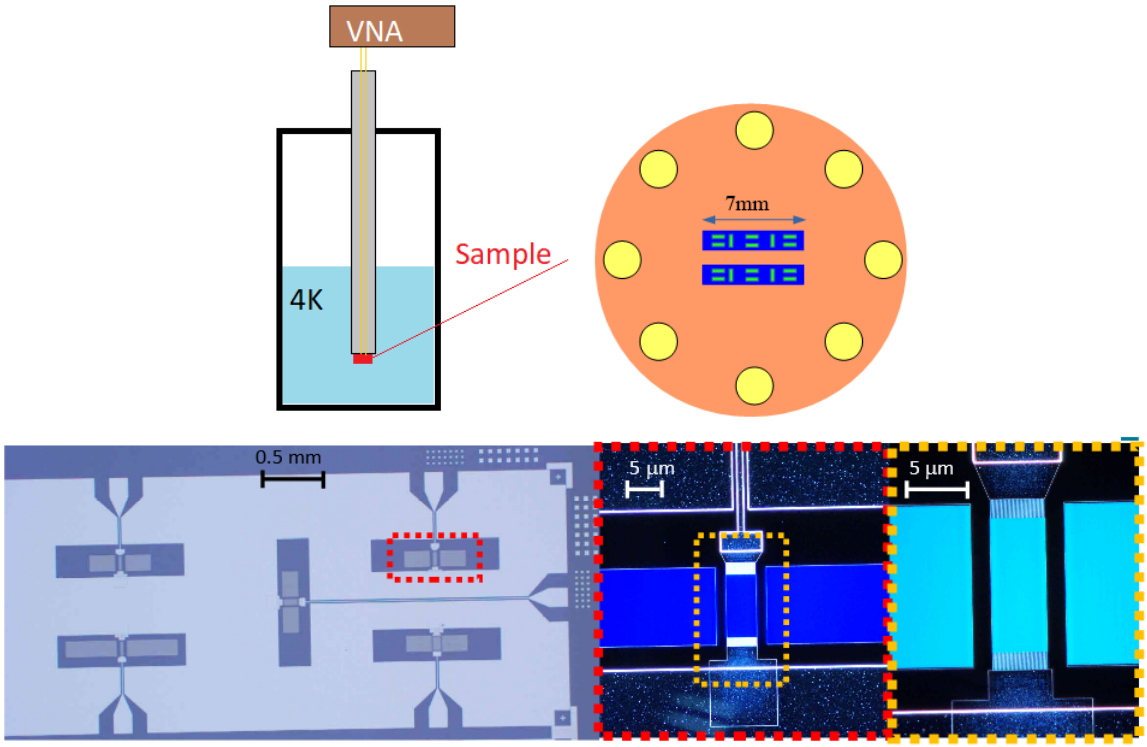

Figure 8: Top: Schematic of the setup and drawing of the sample PCB with the 8 SMP-rf connectors (yellow), the GaAs substrate (blue) and the resonators (green).
Bottom: Optical microscope image at different magnifications of one of the fabricated devices, containing each 8 SAW resonators. The last 2 pictures are taken in dark field modality.

The sample holder with the sample is mounted on a dipstick, which can connect up to 8 different resonators. Inside the dipstick, high frequency coax lines bring the signal from the top connector, where the VNA is then connected, to the resonator.

For the low temperature measurements at 4 K, the dipstick is introduced into a dewar with liquid helium and let to thermalise. One problem that was noticed during the experiments was that keeping the sample fully plunged into the helium would dramatically affect the resonator resonances. This can be easily explained by the mechanical

dumping of the surface acoustic wave standing wave by the liquid helium directly in contact with the GaAs surface [8]. Therefore, the dipstick was introduced into the helium until the SAW resonances started to disappear and then pulled up before performing the measurement. This procedure was repeated every few minutes to ensure that the resonator would still have a temperature $\sim$ 4K in the cold helium gas right above the liquid surface. An alternative approach would use a dipstick with a vacuum chamber, putting the sample into a vacuum and thus disabling the helium from getting in touch with the sample surface.
Each measuring line has to be calibrated in order to reduce the influence in the measurements of standing waves. The results are affected by the fact that the calibration is performed at room temperature, while the device characterization is done in a liquid helium bath at 4K.
The calibration is realized over a range of 500 MHz which allows to take the complete spectrum of the resonator as well as closeups of the different peaks. The number of acquired points of the spectrum is fixed at 20001 points. For the 4K study, an input power of -40 dBm has been used.

3.1 Fitting Function

Following [10], the theoretical reflected power should present a Lorentzian profile, which can be rewritten as a function of the quality factors as follows:

$$S_{11}(f) = A \cdot \frac{\frac{(Q_{ext}-Q_0)}{Q_{ext}} + i2Q_0\delta f}{\frac{(Q_{ext}+Q_0)}{Q_{ext}} + i2Q_0\delta f} \tag{5}$$

where $\delta f = \frac{f-f_0}{f}$ with f_0 the resonance frequency of the resonator. However, quite often, to adapt to experimental phenomena, equation 5 needs to be slightly modified:

$$S_{11\ \text{meas.}}(f) = A \cdot \frac{\frac{(Q_{ext}-Q_0)}{Q_{ext}} + i2Q_0\delta f}{\frac{(Q_{ext}+Q_0)}{Q_{ext}} + i2Q_0\delta f} \exp i\phi + x + iy \tag{6}$$

The introduced phase factor is mainly necessary to fit the asymmetries arising in the shape of the peaks. The origin of this shape is not exactly clear, but they might be related to an interaction of the resonance with the standing waves in the coax lines. [10]

Preferably, one would fit the complex S11 function, but these fits are very sensitive to the quality of the measurements and so this is only really possible at very low temperatures. Instead, fitting the power $|S_{11}|$ allows for a characterization at any temperature. The fit is a least-square optimization returning the optimal parameters and their standard deviations. One of the main difficulties here is to find appropriate starting values for the fit, as its convergence is highly depends on it.
With this fitting procedure, the fitting function is symmetric under exchange of the two quality factors, but it is still possible to distinguish between the internal and the external quality factor by making use of the phase jump at the resonance. If $Q_{ext} > Q_0$, the resonator is undercoupled and the phase jump at the resonance will be smaller than

2π. On the other hand, if $Q_0 > Q_{ext}$, the device is overcoupled and the phase jump is 2π. In most of the cases, surface acoustic wave resonators analysed in this report are undercoupled.

For the room temperature characterization, as the thermal broadening was large enough to make the resonance peaks influence each other, a sum of three terms of the form of equation 5 were added together to perform the fit. In the figures, only the quality factors of the main peak are quoted. At 4K, multiple peaks are fitted separately and the quality factors of each peak are reported. This also gives an idea if the quality factors change between different peaks.

4 Results and Discussion

First, a global overview of the resonator spectrum is measured to give a general view of the resonances for a certain parameter range. For the fits, the data is saved as linear amplitude and phase for closeups over a range of around 20 MHz. The phase jump of the main peak, marked by a coloured dot nearby in the figures, is also plotted for some of the resonators as it allows to distinguish between $Q_0 > Q_{ext}$ and $Q_0 < Q_{ext}$.
In the labels on the plots, λ_0 is replaced by l, p designates the microwave input power and Df is the total linewidth of the resonance. Qe is the external, $Q0$ the internal quality factor and f the resonance frequency of the peak extracted from the fit. In the phase plots, $D\phi$ represents the phase jump around the resonance. In the tables, the numbers 1 and 2 designate respectively the quality factors from the main and the second peak.

4.1 Study of the effect of the mirror spacing d

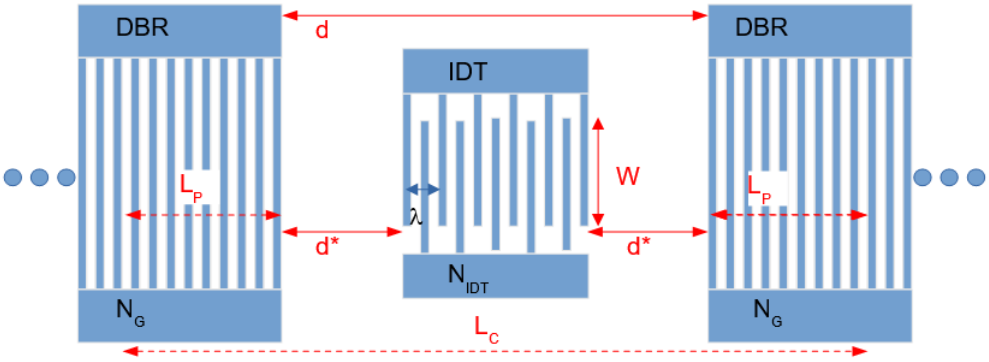

Figure 9: Resonator parameter definition

In the first part, the dependence of internal and external quality factor is studied as a function of the mirror spacing. This not only gives a general feeling for the order of magnitude the quality factors reachable with such SAW resonators, but also allows to fit these data to get the reflection coefficients of the mirrors for an individual finger.

N_{IDT}	79					
N_G	1000					
λ_0	700nm					
d	Variable					
W	$100\lambda_0$					
Quality factors at 4K						
$d[\lambda]$	61	101	201	301	401	501
Q_0 1	4778	7209	13063	10345	13778	15192
Q_{ext} 1	5486	9491	13126	10346	16253	16886
Q_0 2	N/A	6434	11384	9562	11381	12360
Q_{ext} 2	N/A	10216	11387	9759	11437	13991
Peak separation	N/A	55 MHz	22 MHz	16 MHz	13 MHz	7 MHz
Quality factors at RT						
$d[\lambda]$	61	101	201	301	401	501
Q_0	651	2237	3566	888	1051	1381
Q_{ext}	4009	36011	5823	6865	21652	12911

Table 4: Properties of Sample

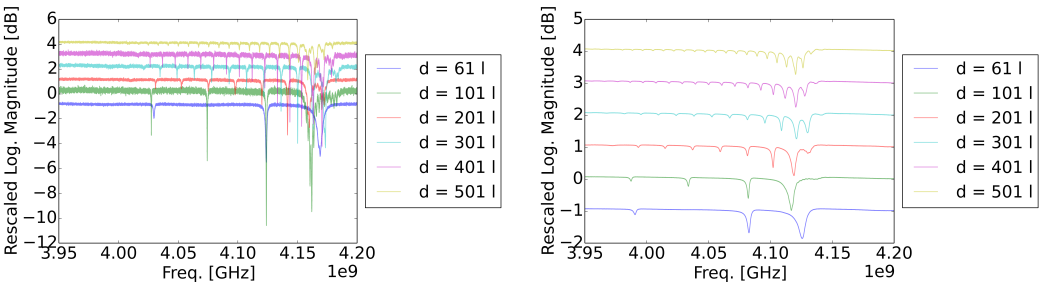

4K Room Temperature

Figure 10: Complete SAW resonator spectrum for different cavity mirror spacings (4K and RT). The different spectra are shifted along y for clarity.

d [um]	Δf [MHz]	L_C [um]
70.7	55	26
140.7	22	65
210.7	16	89.5
280.7	13	110
350.7	8	179

Table 5: Mirror spacing and total cavity length from naive free spectral range formula. The extracted data refers to measurements at 4K reported in Fig. 10

Using the equation for the free spectral range, $\Delta f_d = \frac{v_{SAW}}{2L_C}$, one can now estimate the total cavity length and try to extract r_S from it. The peak separation was easily obtainable as multiple resonance peaks were recorded and their peak frequency precisely determined. But something is wrong. The cavity length extracted in this way is smaller than the actual mirror spacing in the resonators, see table 5. The reason for this is that the single-finger transducer creates a large amount of mechanical reflections. These effectively decouple the cavity into two halves, each having a mirror spacing of d^*.

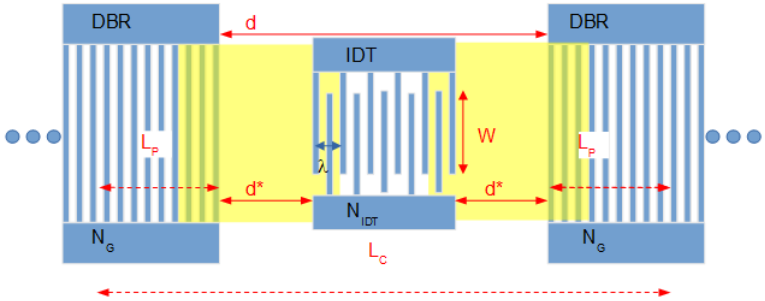

Figure 11: Resonator parameter definition with the two effective cavities marked in yellow, decoupled by the mechanical reflectionof the single finger IDT

Replacing d with d^* in the free spectral range and using the geometric parameters defined in Fig. 3, it can be written as:

$$\begin{aligned} \Delta f &= \frac{v_f}{2L_C} = \frac{v_f}{2(2L_P + d^*)} \\ &= \frac{v_f}{2(2L_P + \frac{d-d'}{2})} \\ \rightarrow \frac{1}{\Delta f} &= \frac{4L_P + d}{v_f} - \frac{0.5N_{IDT} + 0.25}{f} \end{aligned} \tag{7}$$

One can now fit this reciprocal separation against the mirror spacing d, see Fig. 9, to get an estimate for the reflection coefficient of a single finger, $\frac{1}{\Delta f} = \alpha d + \beta$.

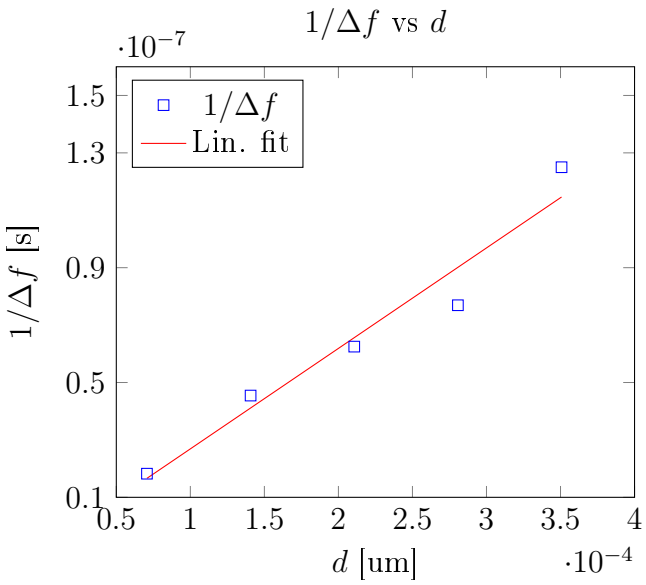

Figure 12: Fit of the peak frequency separation for the different mirror spacings

The fit then gives the following results:
$v_f = 1/\alpha = 2{,}857$ m/s $\rightarrow f = v_f/\lambda_0 = 4.08 \cdot 10^9$ Hz
$L_P = \frac{v_f \beta}{4} + \frac{\lambda}{4}(0.5N_{IDT} + 0.25) = 1.15 \cdot 10^{-6}$ m $= 1.64\lambda_0$
$\rightarrow r_S = \frac{\lambda}{4L_p} = 0.15$
$r_S = 15\%$ is an unrealistic estimate for 30nm Al fingers on GaAs. Indeed, the asymmetry of the effective cavity, with one mirror of N_G fingers and one with N_{IDT} fingers, is not assumed in the model. Some energy is flowing through the IDT instead of getting reflected as was supposed in the derivation of the formula. The sound velocity obtained is very close to the values for bare GaAs found in literature, [1], which is 2864 m/s.

Room Temperature

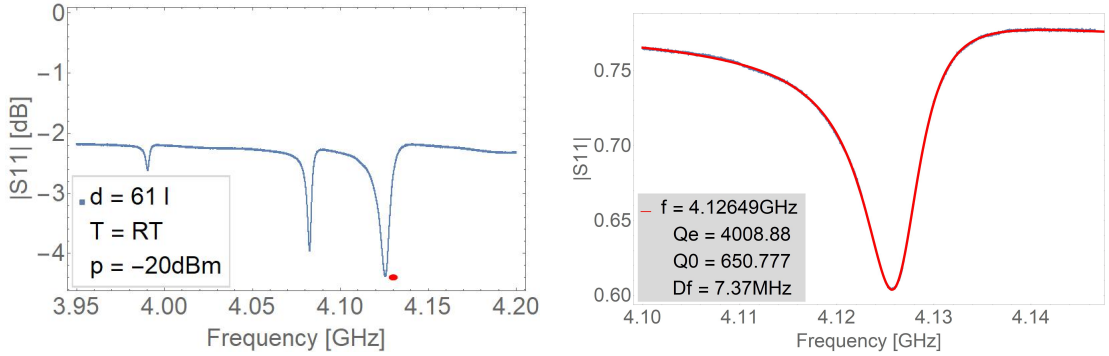

Figure 13: Mirror spacing = 61 λ_0, RT

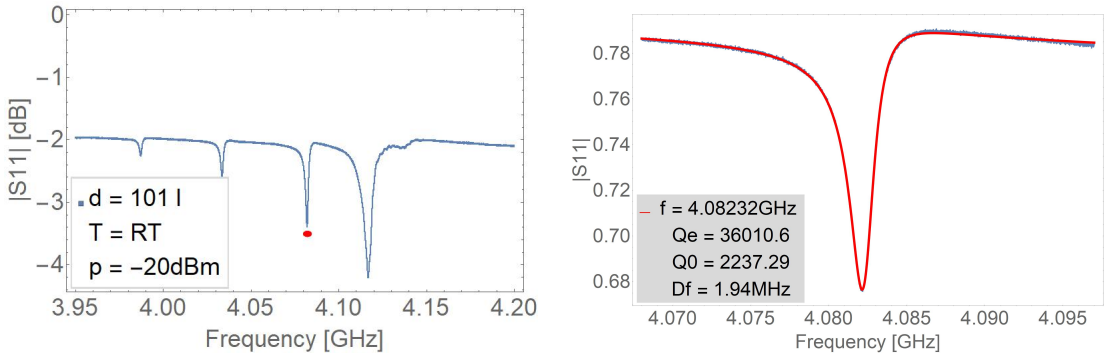

Figure 14: Mirror spacing = 101 λ_0, RT

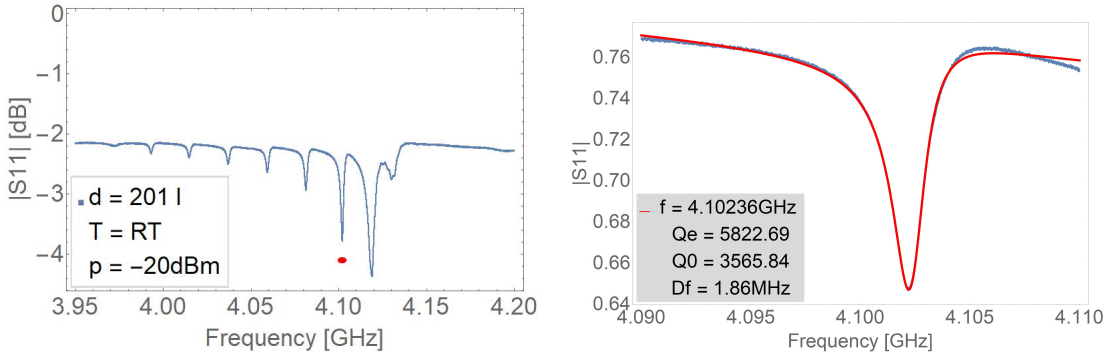

Figure 15: Mirror spacing = 201 λ_0, RT

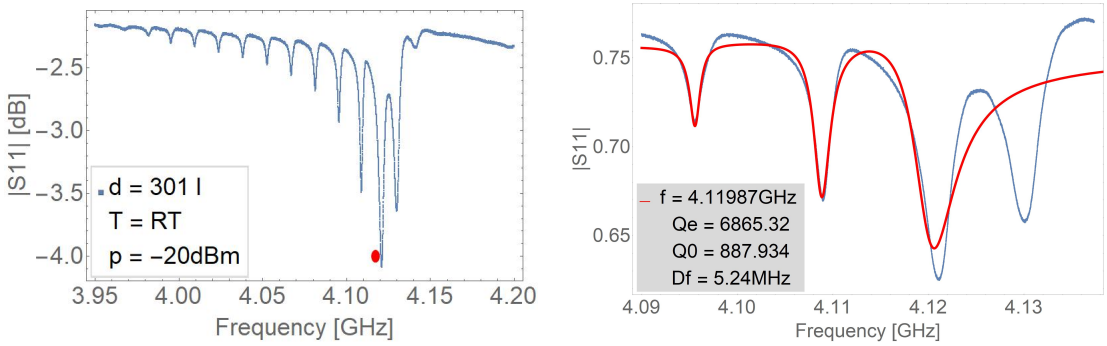

Figure 16: Mirror spacing = 301 λ_0, RT

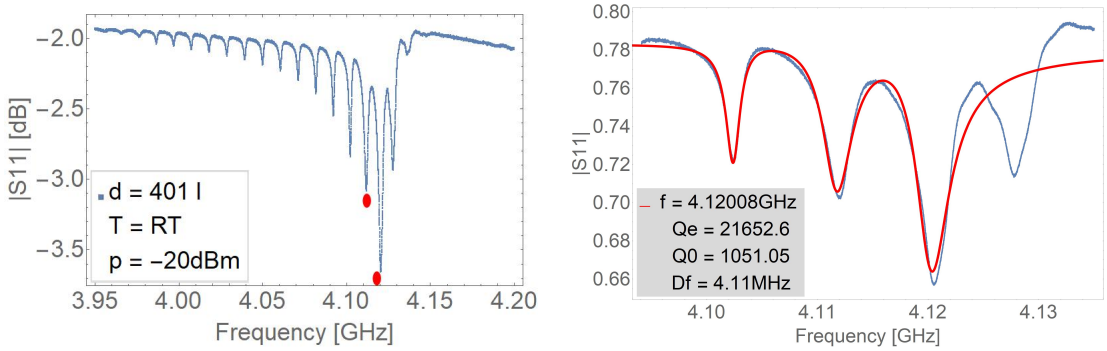

Figure 17: Mirror spacing = 401 λ_0, RT

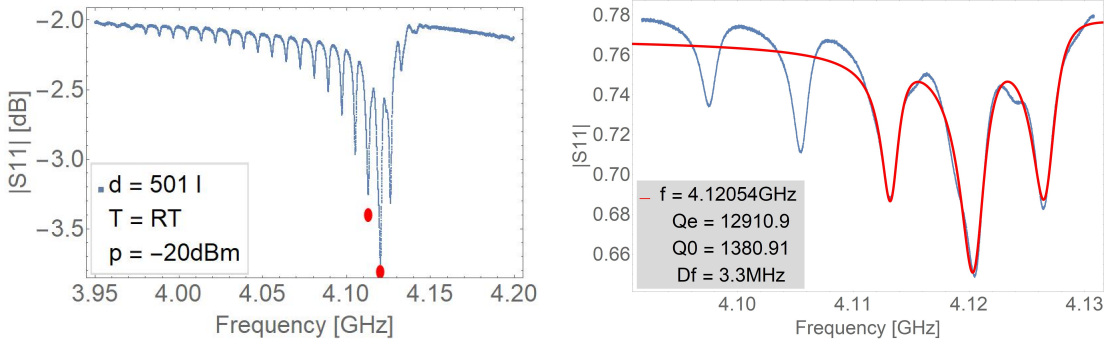

Figure 18: Mirror spacing = 501 λ_0, RT

4K

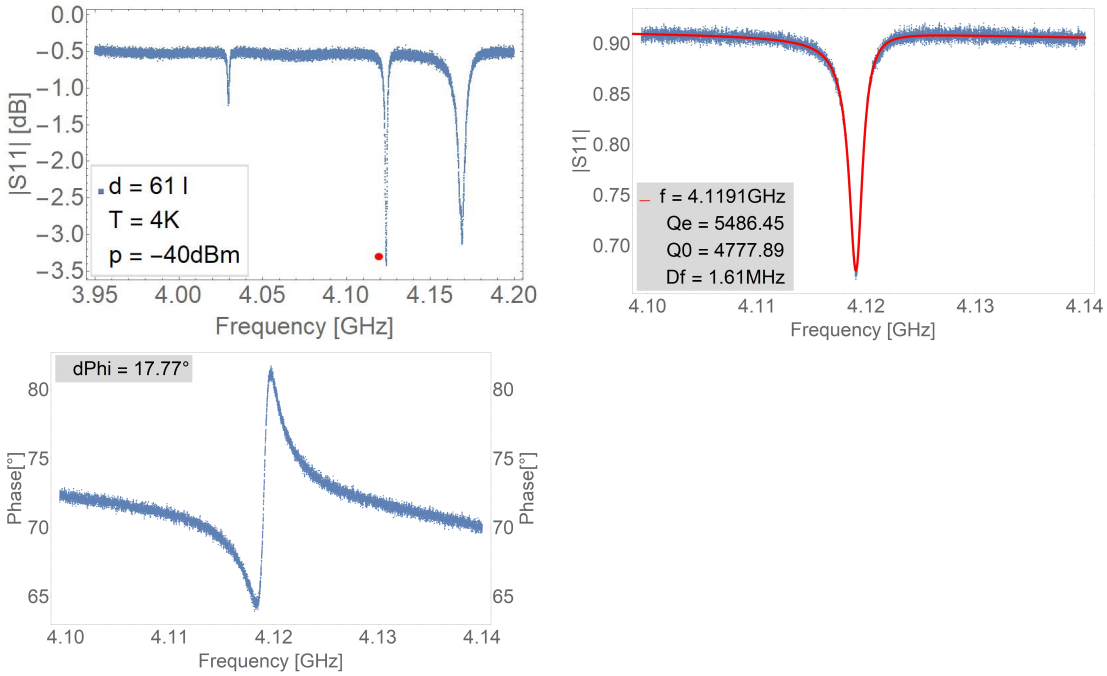

Figure 19: Mirror spacing = 61 λ_0, 4K

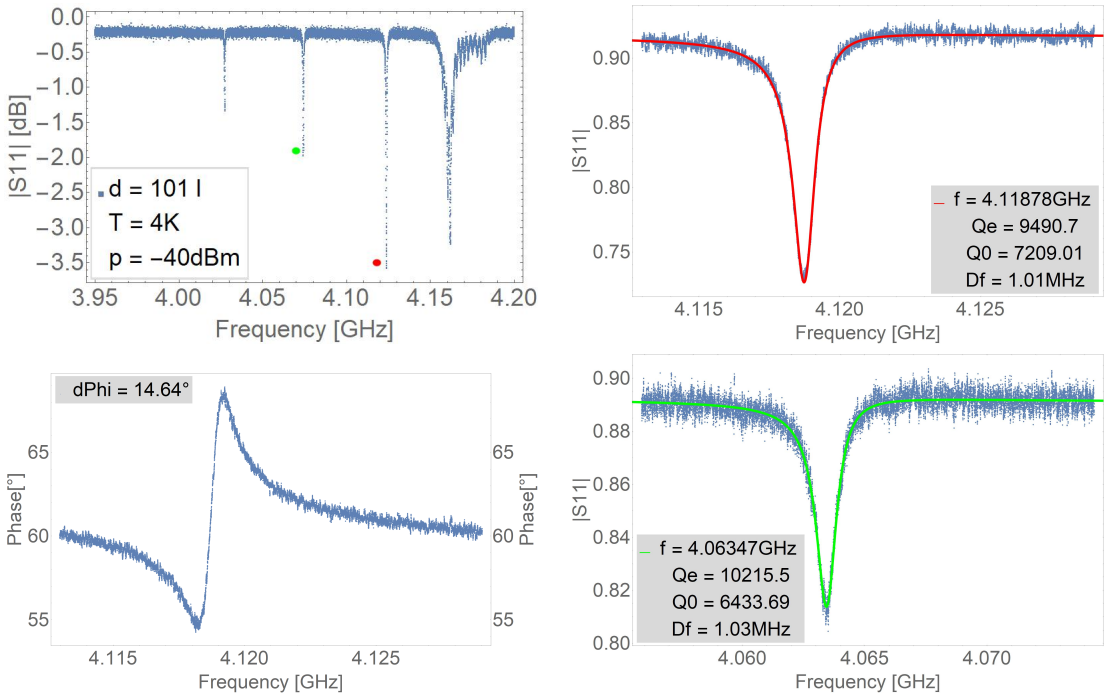

Figure 20: Mirror spacing = 101 λ_0, 4K

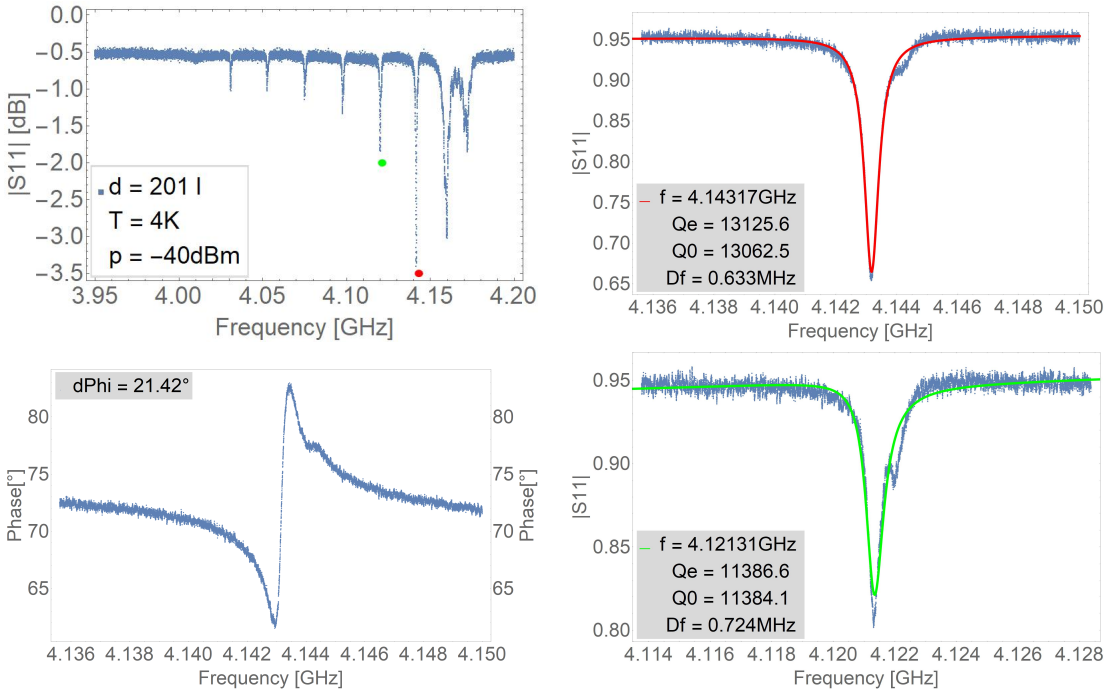

Figure 21: Mirror spacing = 201 λ_0, 4K

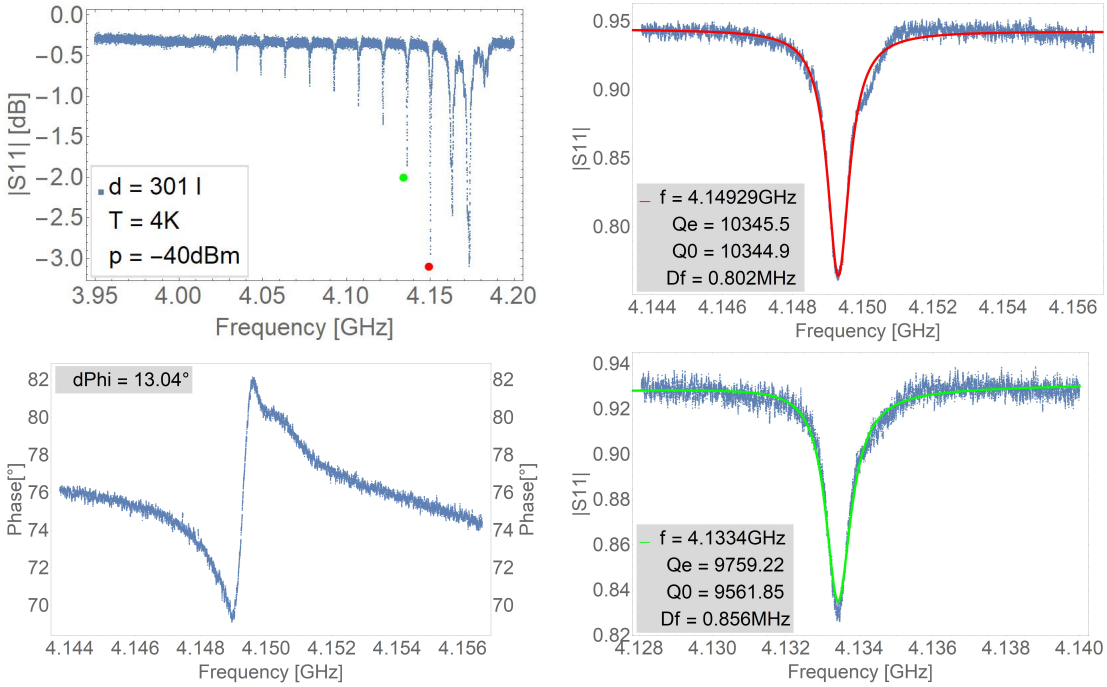

Figure 22: Mirror spacing = 301 λ_0, 4K

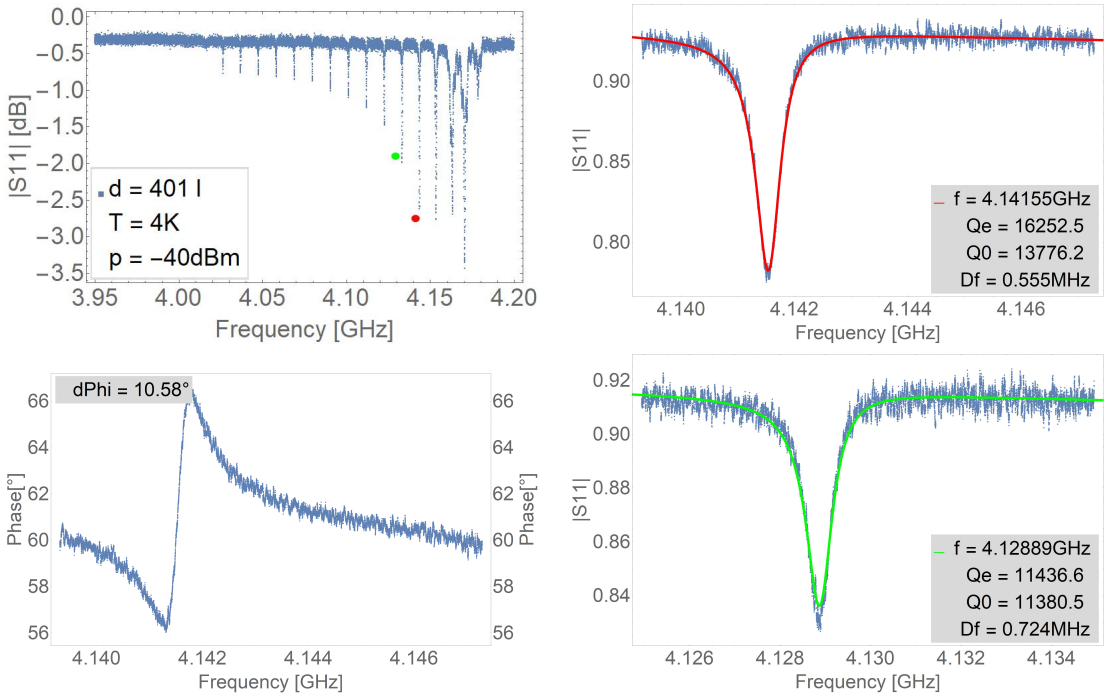

Figure 23: Mirror spacing = 401 λ_0, 4K

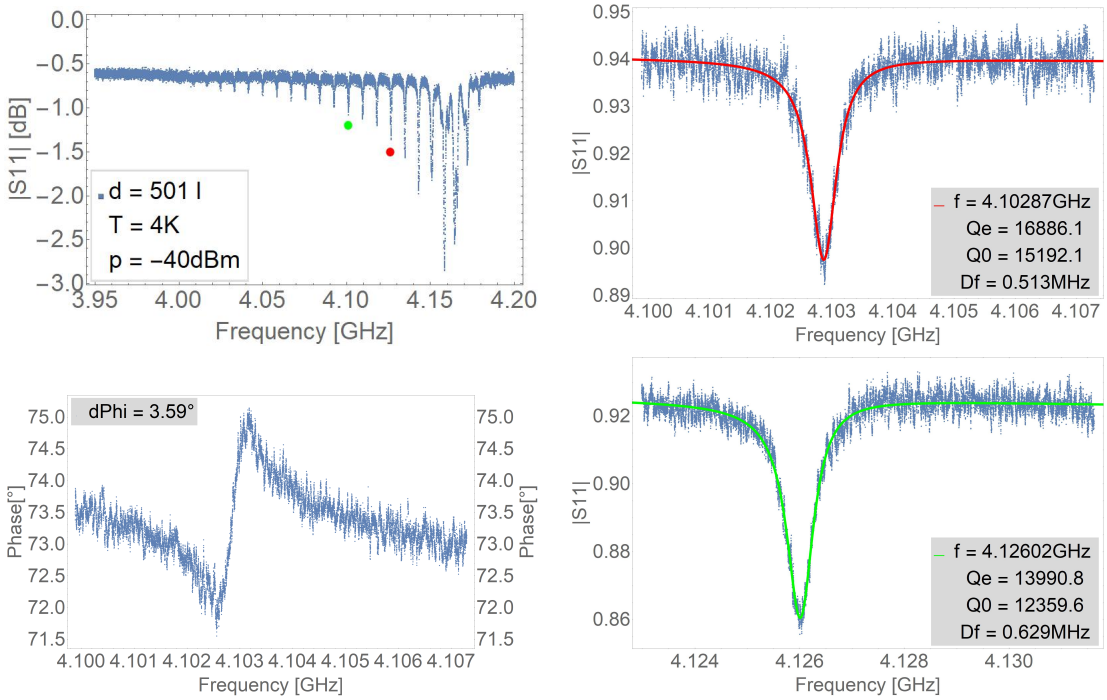

Figure 24: Mirror spacing = 501 λ_0, 4K

4.1.1 Fitting Q_0 as a function of cavity length

As was shown in the previous section, the single-finger transducer decouples the two halves of the cavity. We can make use of eq. (1):

$$Q_0 = \frac{\pi(d + 2L_p)}{\lambda_0(1 - \tanh(|\,r_S\,|\,N_G))}$$

to fit the extracted Q_0 from the main cavity resonance as a function of the cavity length by replacing d with d^*. In this formula, we can express L_P and d^* as a function of the different geometric parameters of the resonator:

$$d^* = \frac{d}{2} - \frac{N_{IDT}\lambda_0}{4}$$
$$L_P = \tanh((N_G - 1)\,|\,r_S\,|)\frac{\lambda_0}{2r_S}$$

In this situation, one has to pay attention to the value of N_G. Its choice is not trivial as the cavity is now asymmetric with different sizes of mirrors on the two ends. This means that the factor $r_s N_G$ is the only quantity that can be correctly determined from the fit.

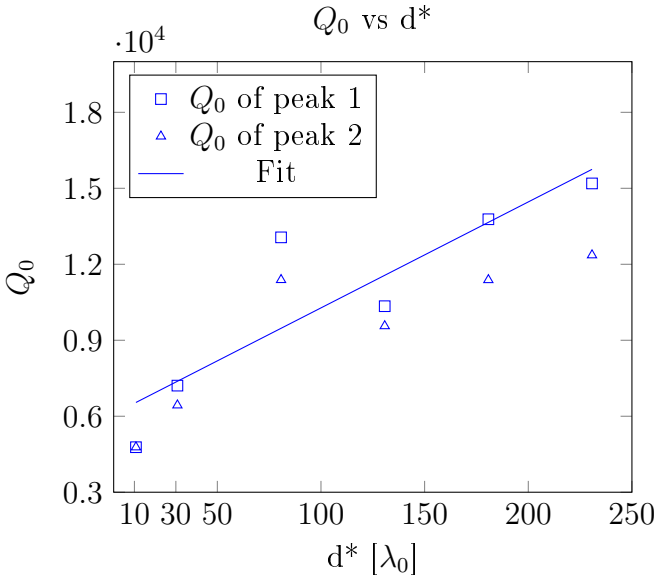

Figure 25: Internal quality factor fitted against spacing between Bragg reflector and IDT

From the fit reported in Fig. 25, one can extract $r_s N_G \simeq 42.77 \pm 10$ and, assuming $N_G = 1000$, we get $r_s = 4.28 \cdot 10^{-2}$ ± 0.01, which seems reasonable given the finger thickness in the devices (30-35nm). This result, of course, does not take into account the asymmetric reflector configuration of the device under the assumption that the IDT decouples the two cavities.

4.2 Study of the effect of the number of fingers in the grating reflector N_G

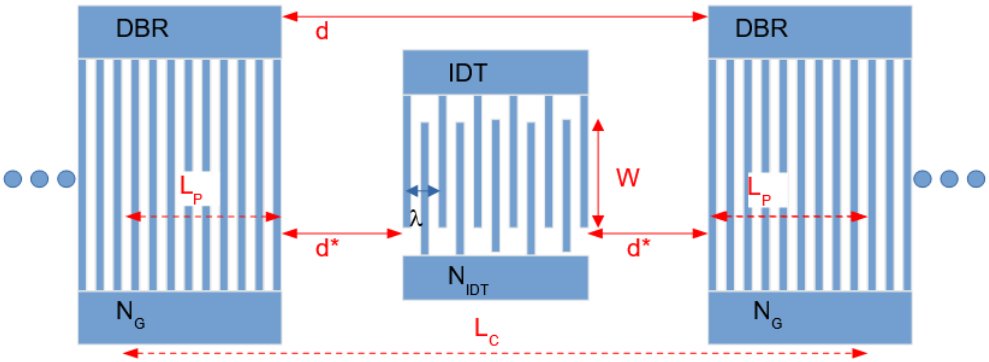

Figure 26: Resonator parameter definition

By changing the number of fingers in the mirror N_G, only the internal quality factor should change and increase with larger number of fingers in the mirror. This should lead us closer to the critical coupling condition. For mirrors composed with a higher number of fingers, the leaking of energy through the IDT becomes more important, which then makes this energy loss the main limiting factor.

N_{IDT}	79 fingers				
N_G	Variable				
λ_0	600 nm				
d	201 λ_0		101 λ_0		
W	100 λ_0				
Quality factors at 4K					
N_G	500	1000	500	1000	1500
Q_0 1	16271	13959	8912	9334	4790
Q_{ext} 1	18395	14889	12927	11064	9805
Q_0 2	16689	14786	13199	3325	4264
Q_{ext} 2	15453	16632	13231	7591	11893

Table 6: Properties of Sample

The results presented in table 6 do not show a clear trend towards higher internal quality factors as would be expected from equation (1). This can be explained by the mechanical reflections in the single finger IDT. Considering only the decoupled half of the cavity, this series is changing only the reflector on one side of the cavity, which is already a lot larger than the effective reflection coefficient on the other side of the cavity, given by the reflections in the single-finger IDT. The amount of energy leaking through

the transducer is more important, but the number of fingers in the IDT stays constant through the 3 devices, so Q_0 remains limited by the reflection coefficient of the IDT.

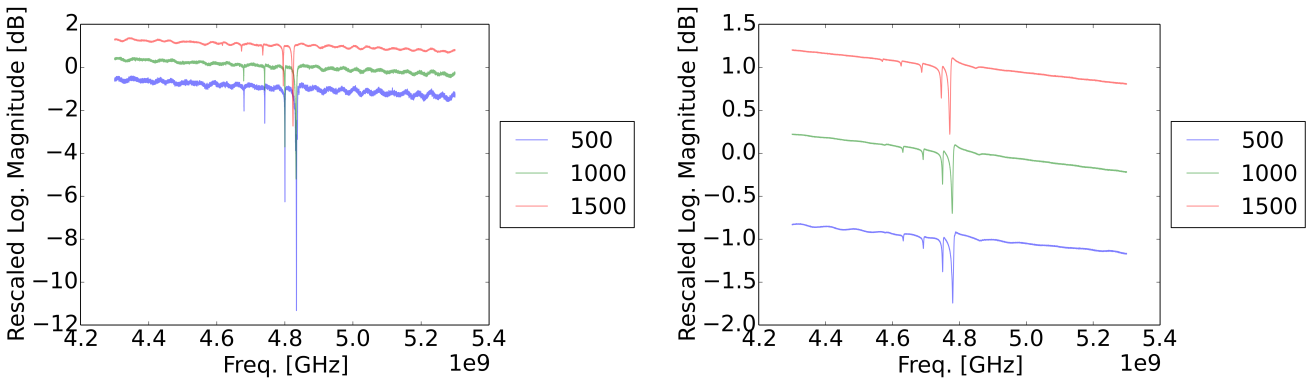

4K Room Temperature

Figure 27: Complete spectrum, different mirror sizes at 101 λ_0 mirror spacing, 4K and RT

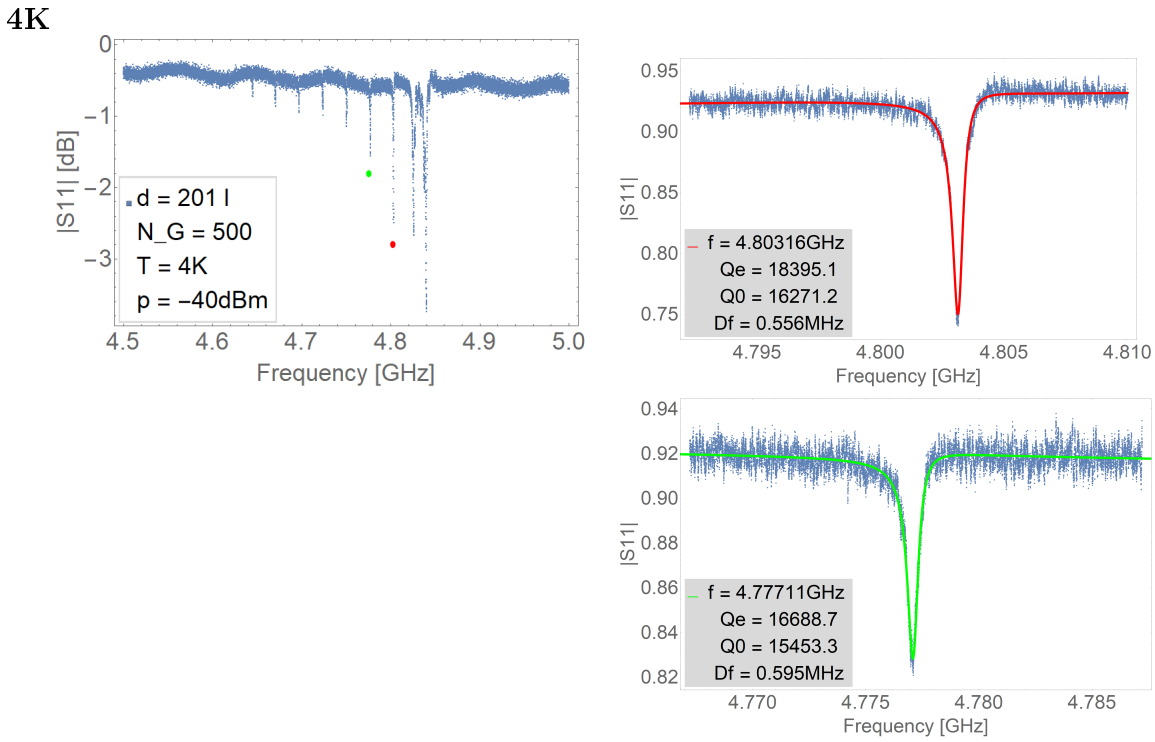

Figure 28: Mirror spacing = 201 λ_0, number of fingers in the grating = 500, 4K

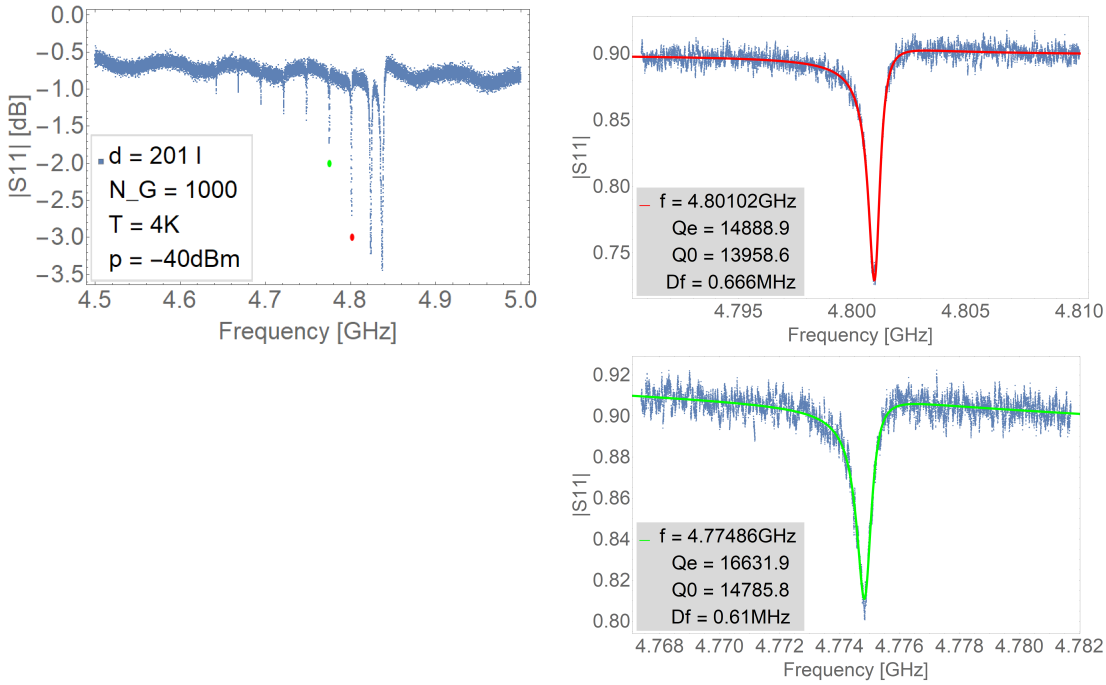

Figure 29: Mirror spacing = 201 λ_0, number of fingers in the grating = 1000, 4K

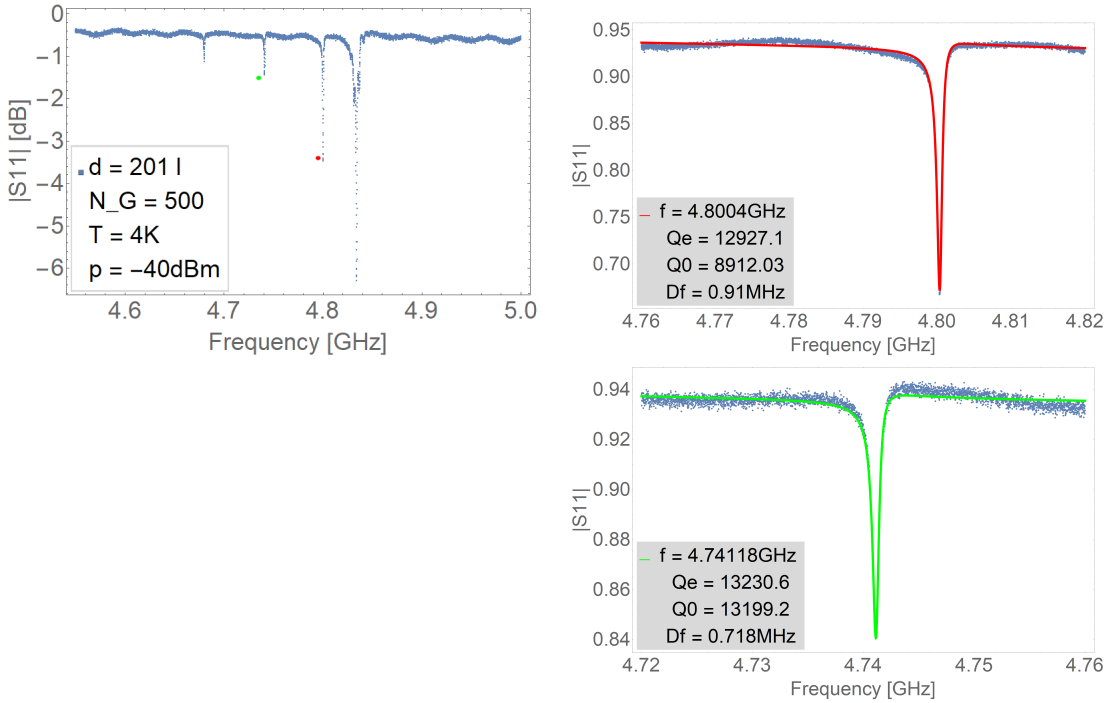

Figure 30: Mirror spacing = 101 λ_0, number of fingers in the grating = 500, 4K

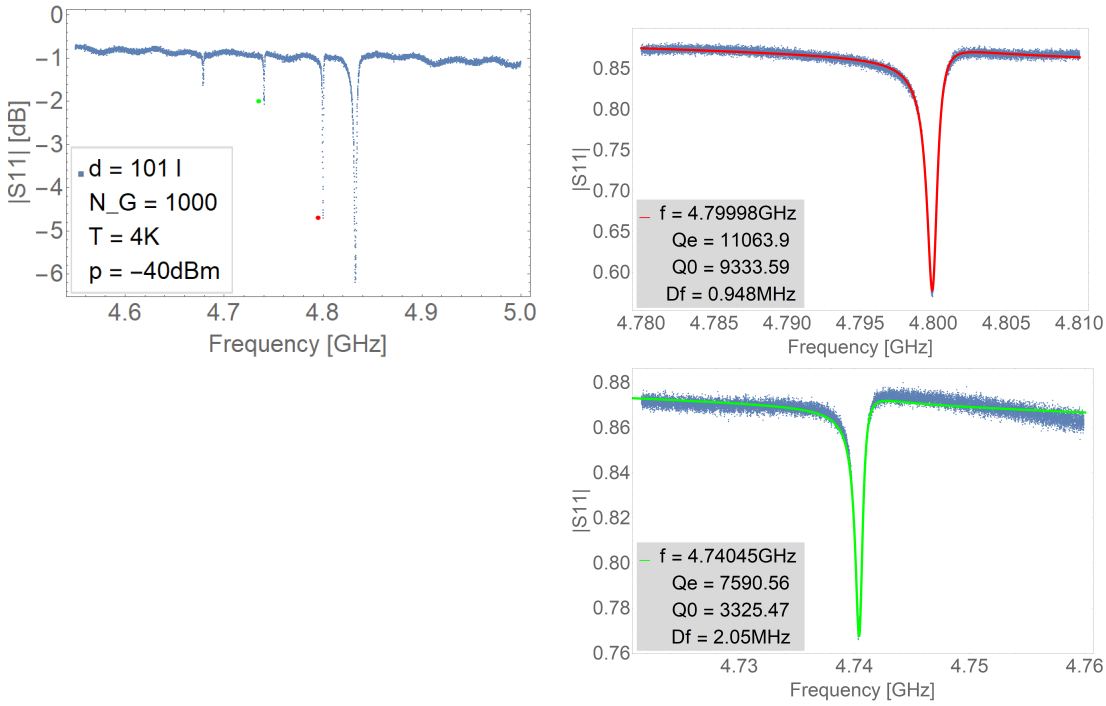

Figure 31: Mirror spacing = 101 λ_0, number of fingers in the grating = 1000, 4K

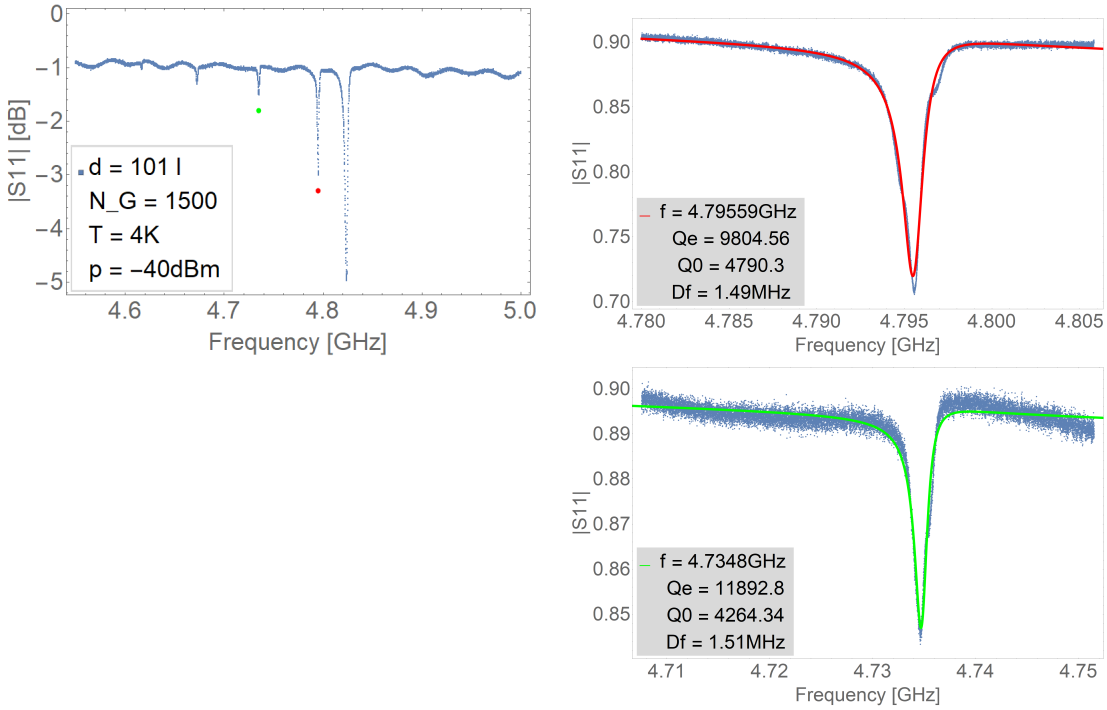

Figure 32: Mirror spacing = 101 λ_0, number of fingers in the grating = 1500, 4K

4.3 Study of the effect of the cavity width W

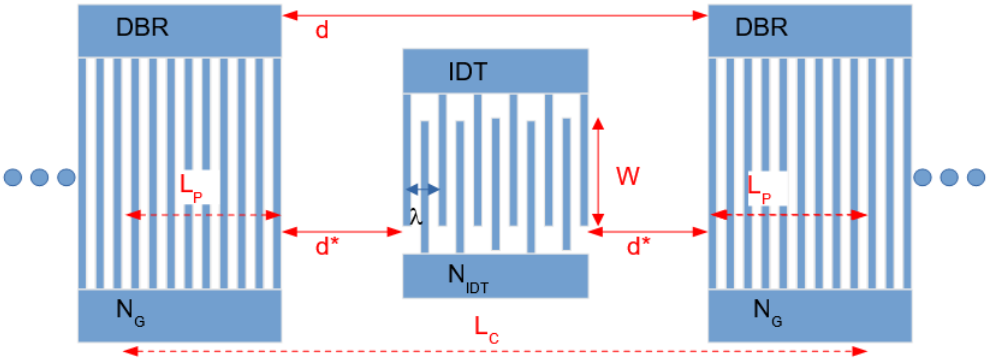

Figure 33: Resonator parameter definition

To reduce the external quality factor, one can increase the width of the cavity, which corresponds to making the IDT fingers longer (see Fig. 3). This leads to larger external losses. At very small finger lengths, see eq.(2), it is predicted that diffraction might become the limiting factor for the quality of the resonators. For $W = 25\lambda_0$, the smallest width of the tested resonators, the estimate of the internal quality factor due to diffraction loss is 21000, already a factor of 2 higher than the best Q_0 obtained in our study. For $W = 50\lambda_0$, this limit is already 80000, therefore in practice negligible. Following equation (3), the external quality factor should be inversely proportional to the cavity width, $Q_{ext} \propto \frac{1}{W}$. Even though a slight trend is observed in the measured quality factors reported in Fig. 35, the trend does not satisfy the inverse proportionality predicted by the equation. This means that other factors are playing a role that change the external quality factor as well.

N_{IDT}	79 fingers						
N_G	1000						
λ_0	600 nm						
d	201 λ_0						
W	Variable						
$W[\lambda]_0$	200	175	150	125	75	50	25
Quality factors at 4K							
Q_0 1	17038	16515	16088	11460	17410	18988	15200
Q_{ext} 1	17215	16604	16368	11824	18820	19274	15998
Q_0 2	18637	17352	18216	11798	20572	21076	11245
Q_{ext} 2	18655	18280	18278	19509	22063	22924	14471
Diff. Limit	1.3e6	1.0e6	7.6e5	5.3e5	1.9e5	8.5e4	2.1e4

Table 7: Properties of Sample

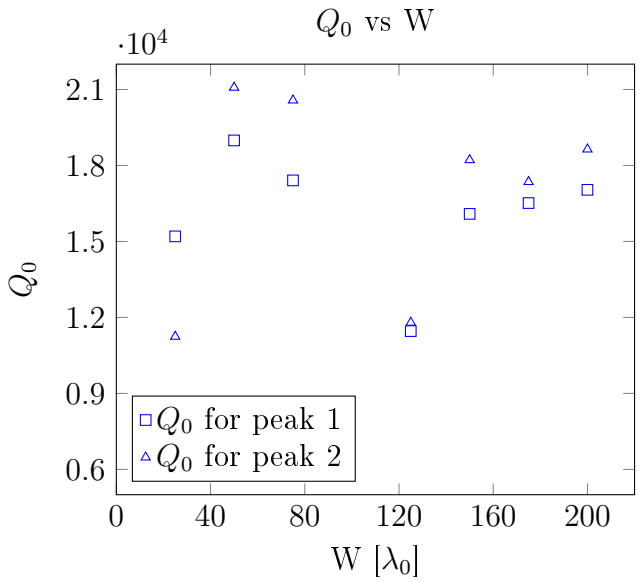

Figure 34: Internal quality factor as a function of cavity width. Even though the trend corresponds to the theory, the dependence on the width is not as pronounced as expected.

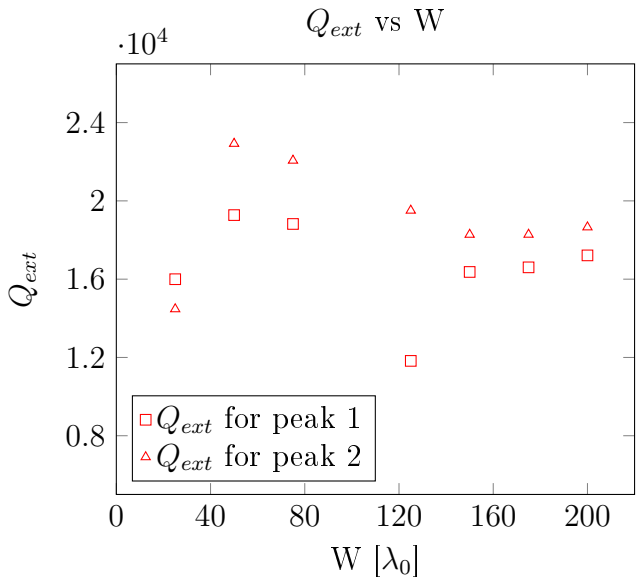

Figure 35: External quality factor plotted against the cavity width.

4K

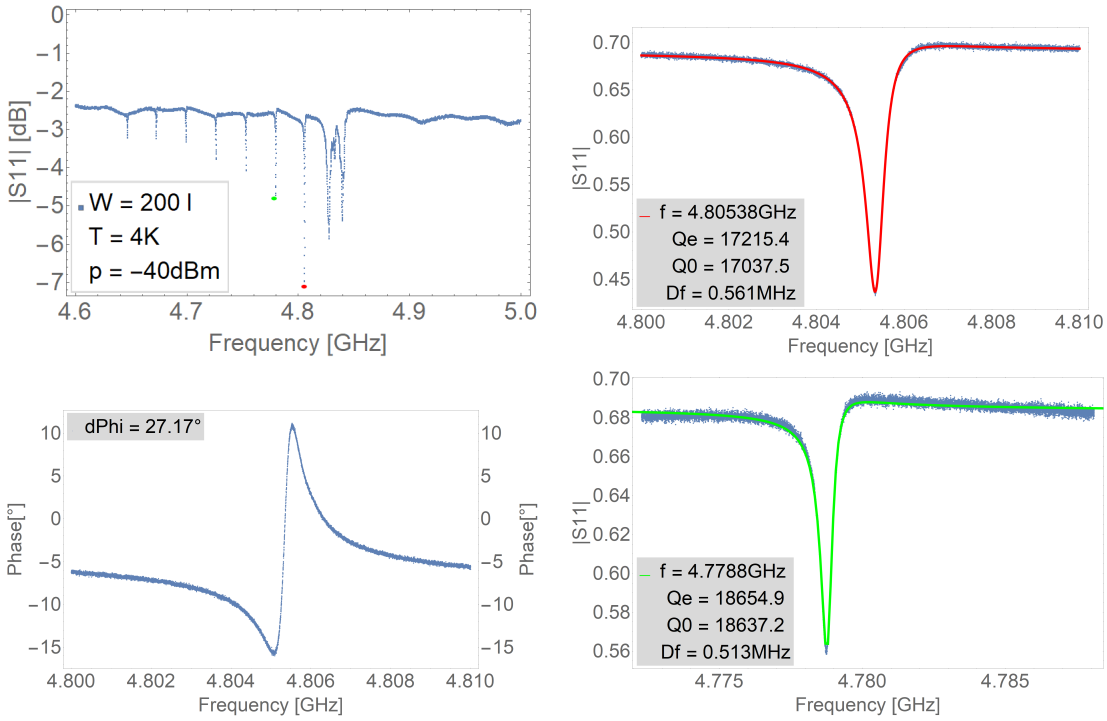

Figure 36: Cavity width = 200 λ_0, 4K

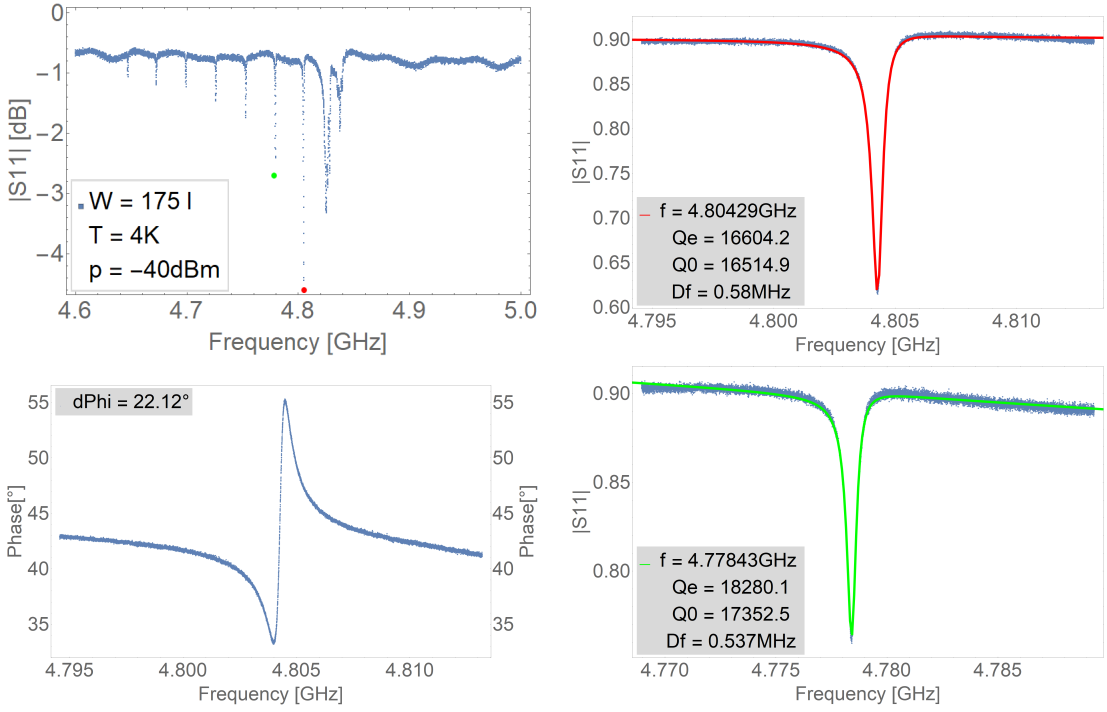

Figure 37: Cavity width = 175 λ_0, 4K

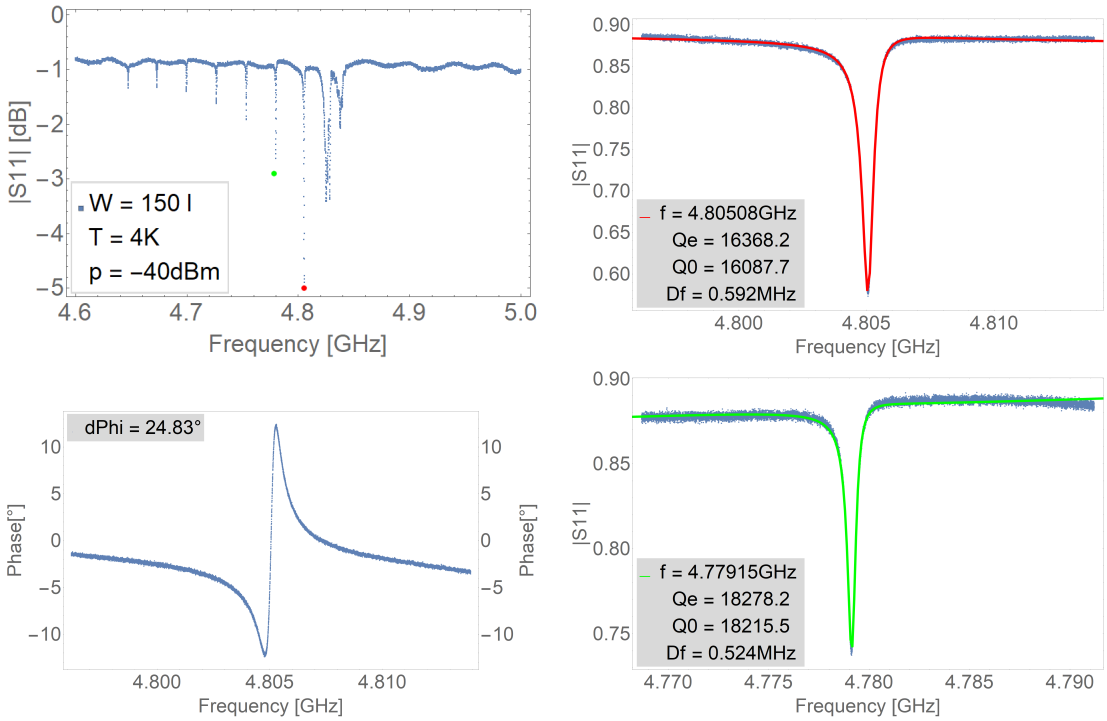

Figure 38: Cavity width = 150 λ_0, 4K

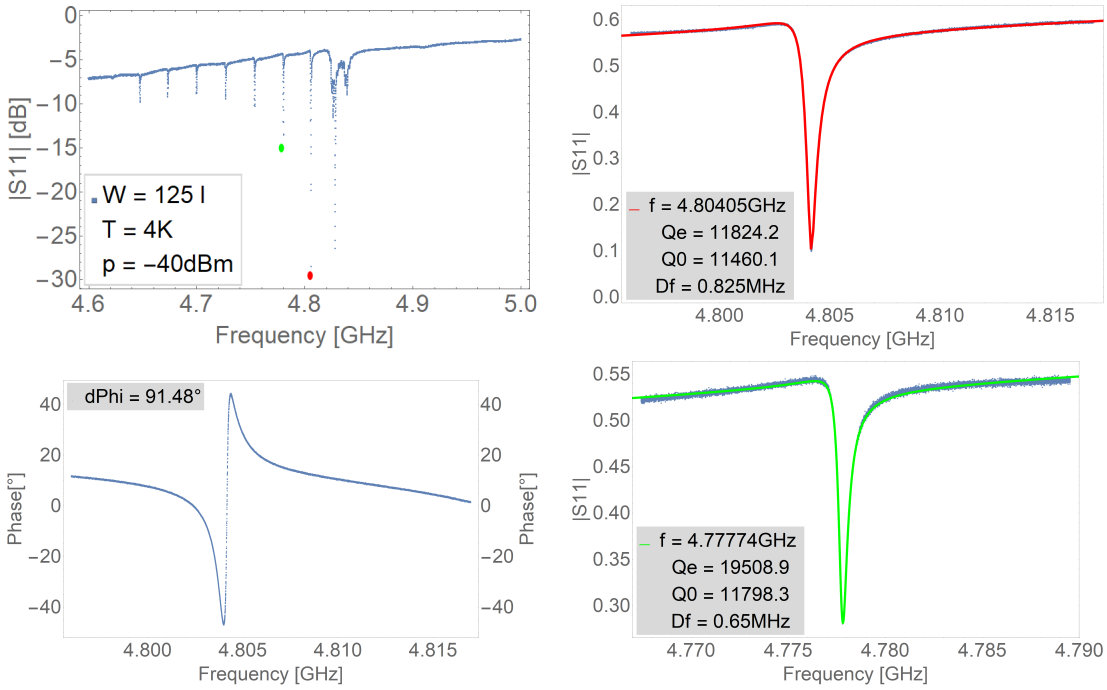

Figure 39: Cavity width = 125 λ_0, 4K

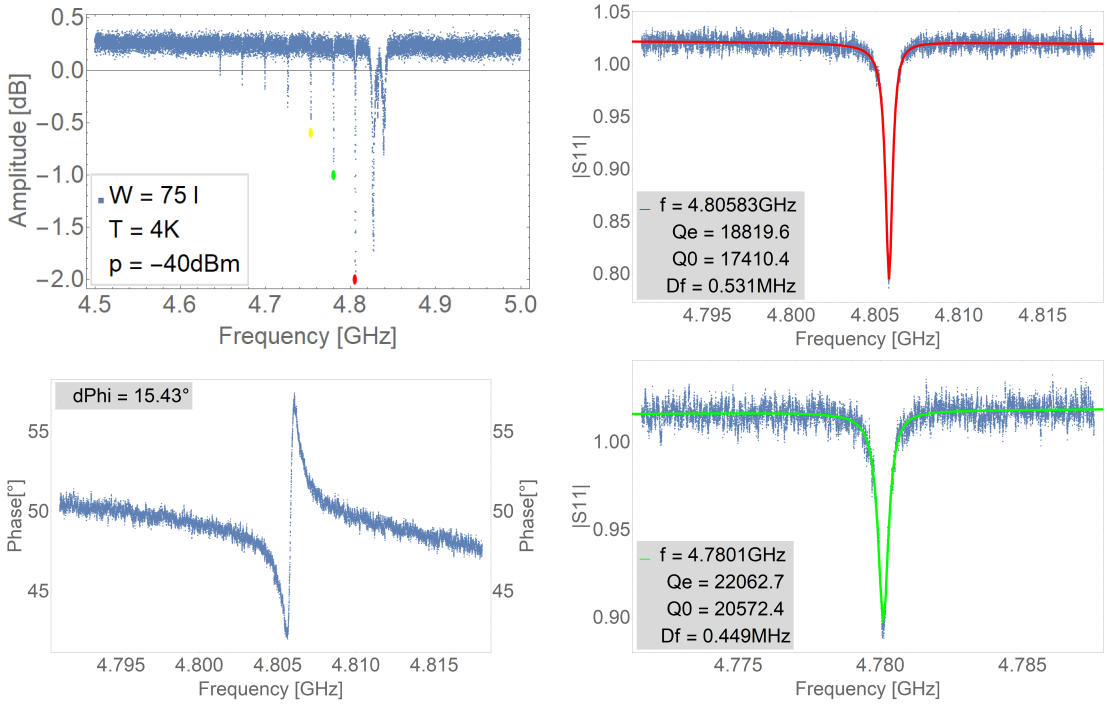

Figure 40: Cavity width = 75 λ_0, 4K

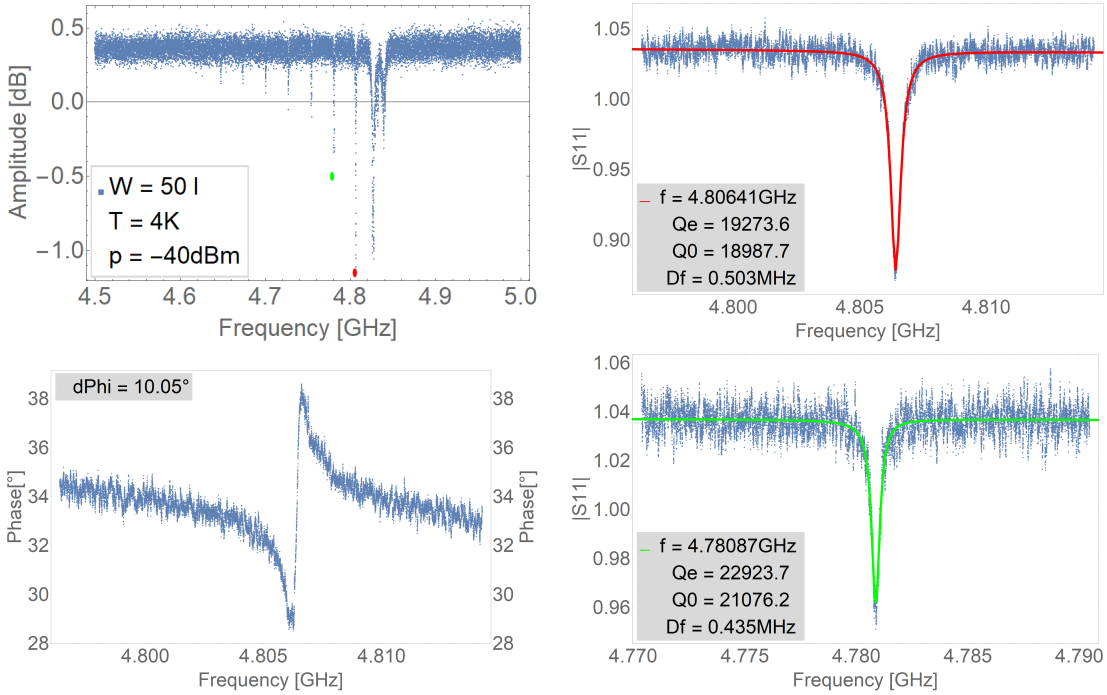

Figure 41: Cavity width = 50 λ_0, 4K

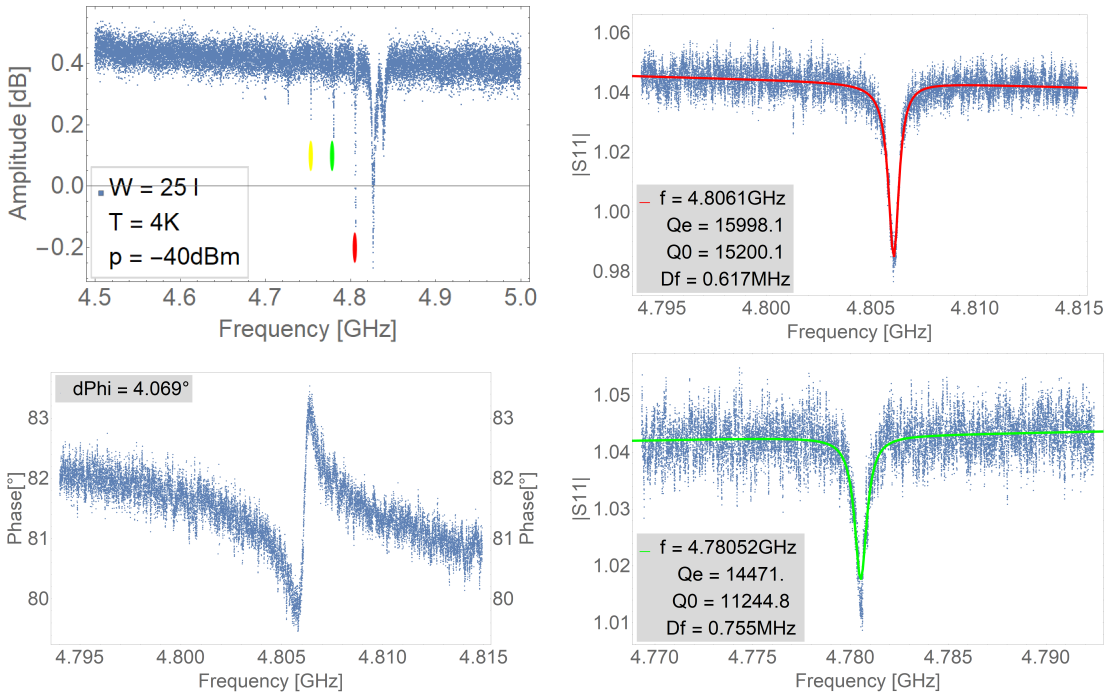

Figure 42: Cavity width = 25 λ_0, 4K

4.4 Study of the effect of the number of fingers in the transducer N_{IDT}

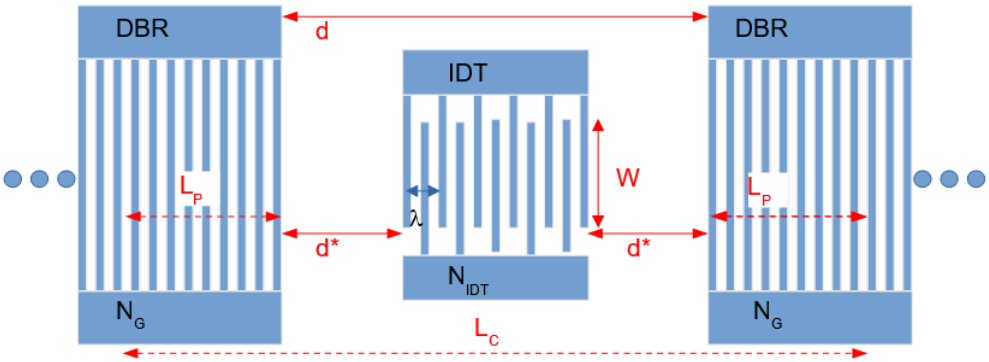

Figure 43: Resonator parameter definition

To better understand the effects of the IDT, especially as some of the previous results suggested that the IDT might decouple the two sides of the cavity for N_{IDT} sufficiently high, a study with varying number of fingers in the tranducer was performed. As seen in equation (3)

$$Q_{ext} \propto \frac{L_C}{N_{IDT}^2}$$

the external quality factor should strongly decrease with an increasing number of fingers in the IDT. The total cavity length, L_C, is important as this is also changing when changing N_{IDT}, if taking into consideration the strong mechanical reflections that occur by the single finger transducer and thus a reduction in the effective mirror spacing d^* (see Fig. 3).

Fig. 45 presents an overview of the extracted Q_{ext} as a function of N_{IDT}. Even though the trend is present in the external quality factor, the fit did not give any reasonable results. Again, it seems that mechanical reflections in the IDT are an important contribution influencing the quality factors.

N_{IDT}	Variable					
N_G	1000					
λ_0	600 nm					
d	101 λ_0					
W	100 λ_0					
N_{IDT}	199	159	119	79	39	19
Quality factors at 4K						
Q_0 1	4230	7075	3124	9349	8858	15183
Q_{ext} 1	4748	3306	5663	9462	9365	16226
Q_0 2	3271	9086	8649	10847	8566	16662
Q_{ext} 2	5301	4875	9457	11223	10881	17119
Δf	N/A	0.12	0.09	0.059	0.052	0.044

Table 8: Properties of Sample

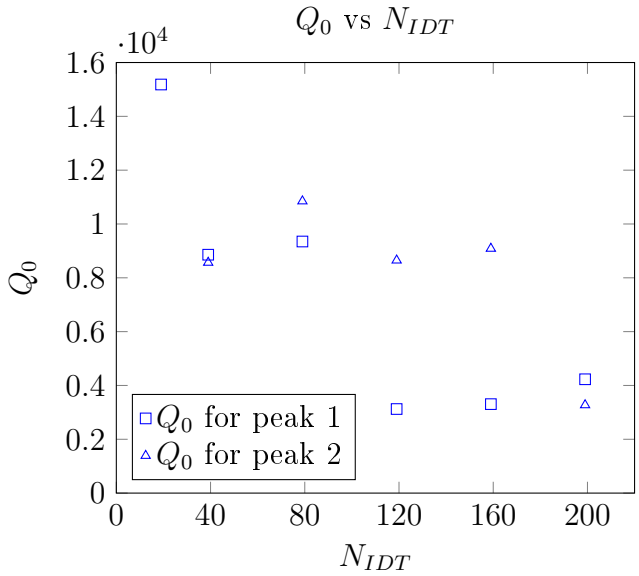

Figure 44: Internal quality factor as a function of the number of fingers in the transducer

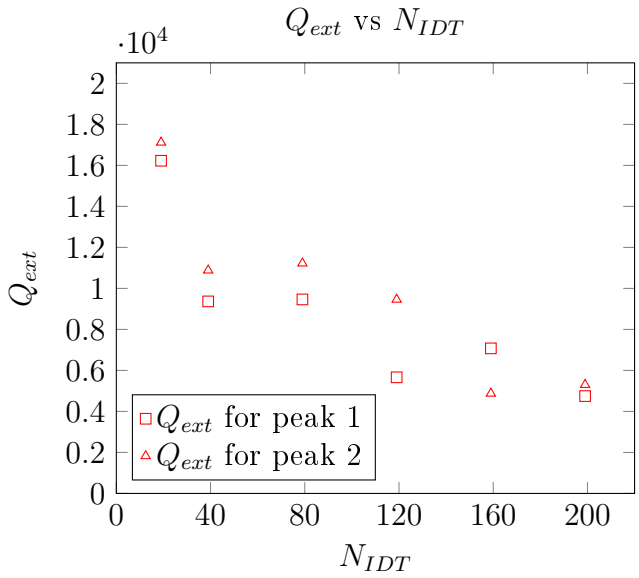

Figure 45: External quality factor as a function of the number of fingers in the transducer

Making use of equation (7), developed in the theory part for two decoupled cavities, one can extract the reflectivity of a single finger by fitting the peak frequency separation Δf of the resonance peaks at different numbers of fingers in the transducer:

$$\frac{1}{\Delta f} = -\frac{1}{f}\left(0.5N_{IDT} + \frac{1}{4}\right) + \frac{4L_P + d}{v_f} \tag{8}$$

$$= \alpha\left(0.5N_{IDT} + \frac{1}{4}\right) + \beta \tag{9}$$

One can determine the frequency, the velocity of the waves and the reflectivity of the fingers in the mirror from the penetration depth of the surface acoustic wave by performing a linear fit according to eq. (9), as reported in Fig. 3. The separation of the peaks is determined again by performing the characterisation on multiple peaks and thus receiving precise data on the exact position of the peak.

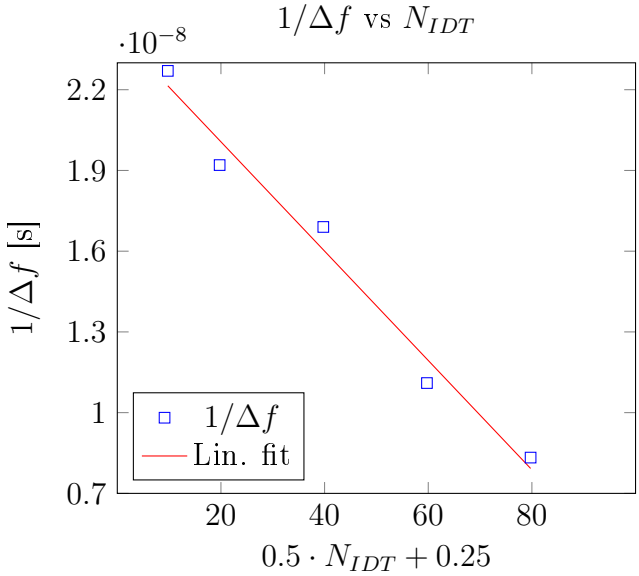

Figure 46: Fit of the peak separation as a function of number of fingers in the IDT

The results obtained are the following:
$f = -\frac{1}{\alpha} = 4.92 \cdot 10^9$ Hz $\rightarrow v_f = \lambda_0 \cdot f = 2{,}953.8$ m/s
$L_P = \frac{v_f\beta - d}{4} = 2.67 \cdot 10^{-6}$ m $= 4.44\lambda_0$.
Using the expression, $L_P = \frac{\tanh((N_G-1)r_S)\lambda_0}{4r_S}$, one can extract $r_S = 5.63 \cdot 10^{-2} \pm 0.01$. This result is similar to the estimate for $\mid r_S \mid$ from fitting the quality factors as a function of mirror spacing, as has been done in section 4.1.1. Therefore, the reflectivity is probably around 5% for Al fingers as used in this project. The surface sound velocity obtained is also similar to the data provided in other sources, for example in [1] 2864 m/s is given as the sound velocity of GaAs.

4K

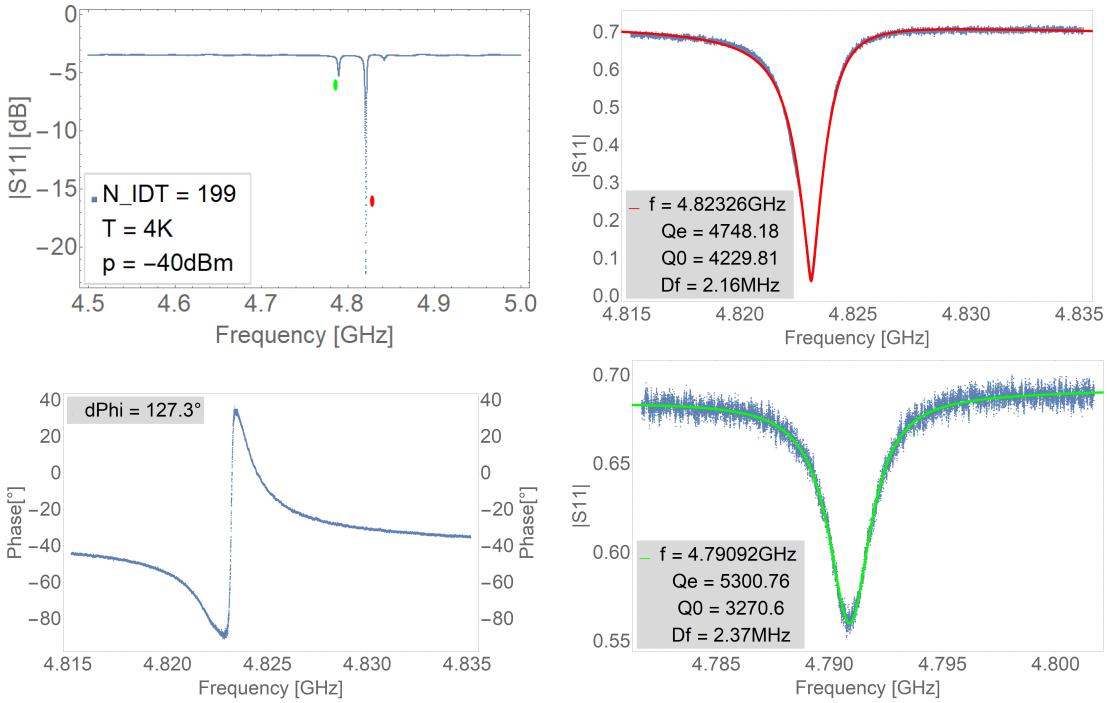

Figure 47: Number of fingers in the IDT = 199, 4K

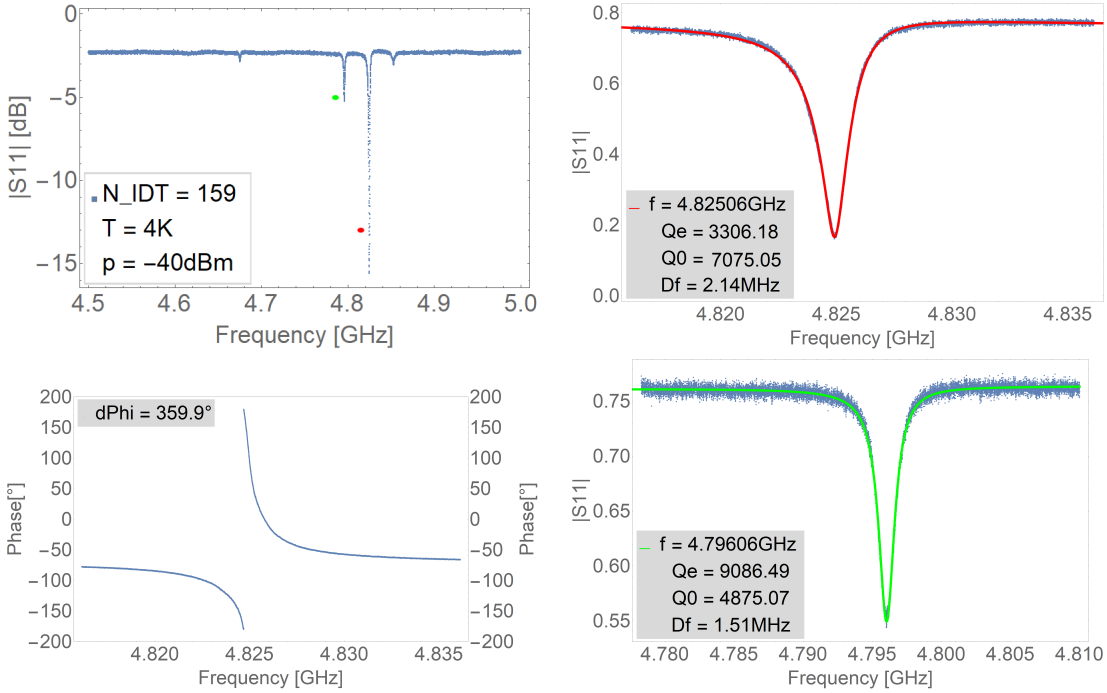

Figure 48: Number of fingers in the IDT = 159, 4K

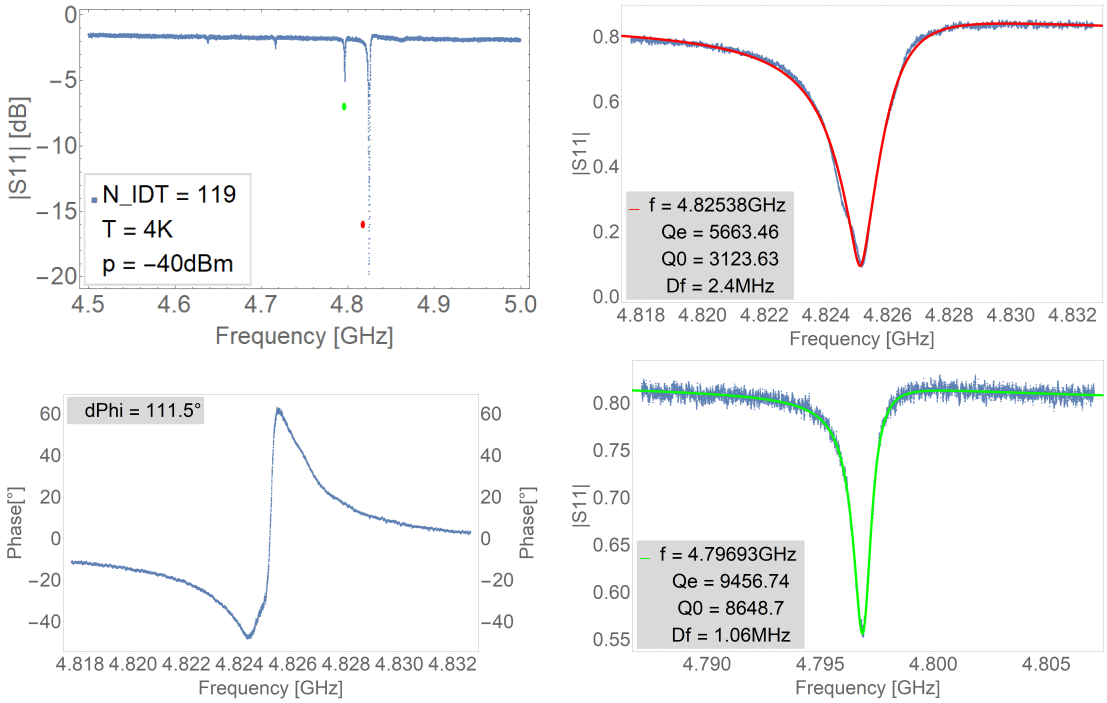

Figure 49: Number of fingers in the IDT = 119, 4K

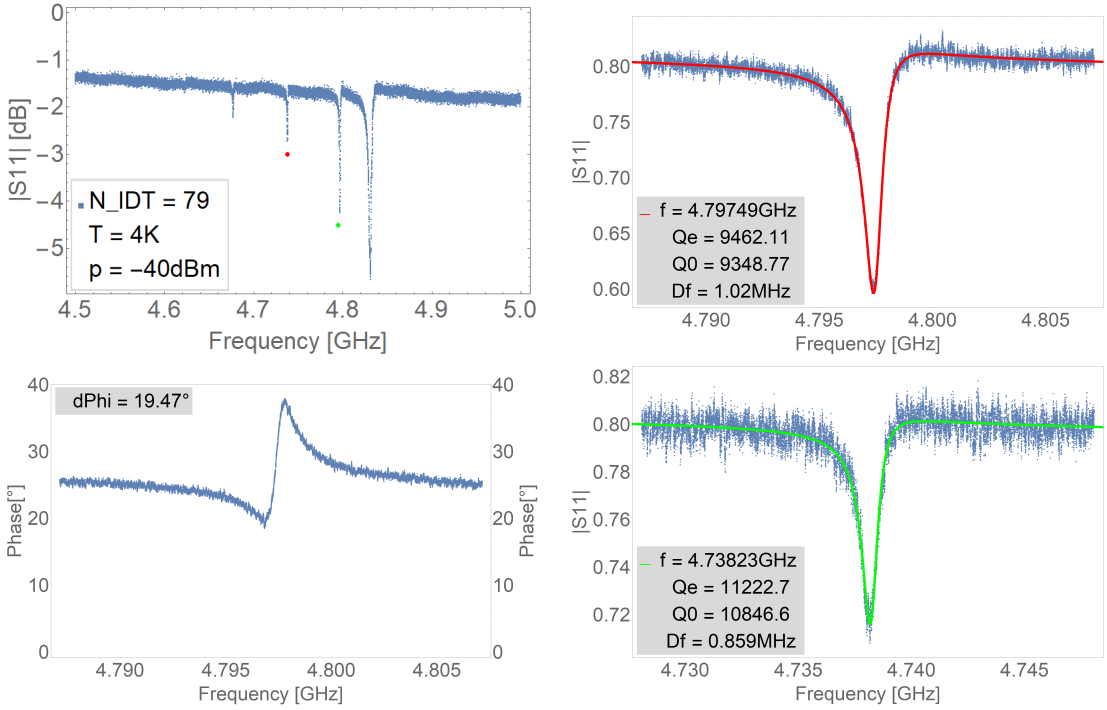

Figure 50: Number of fingers in the IDT = 79, 4K

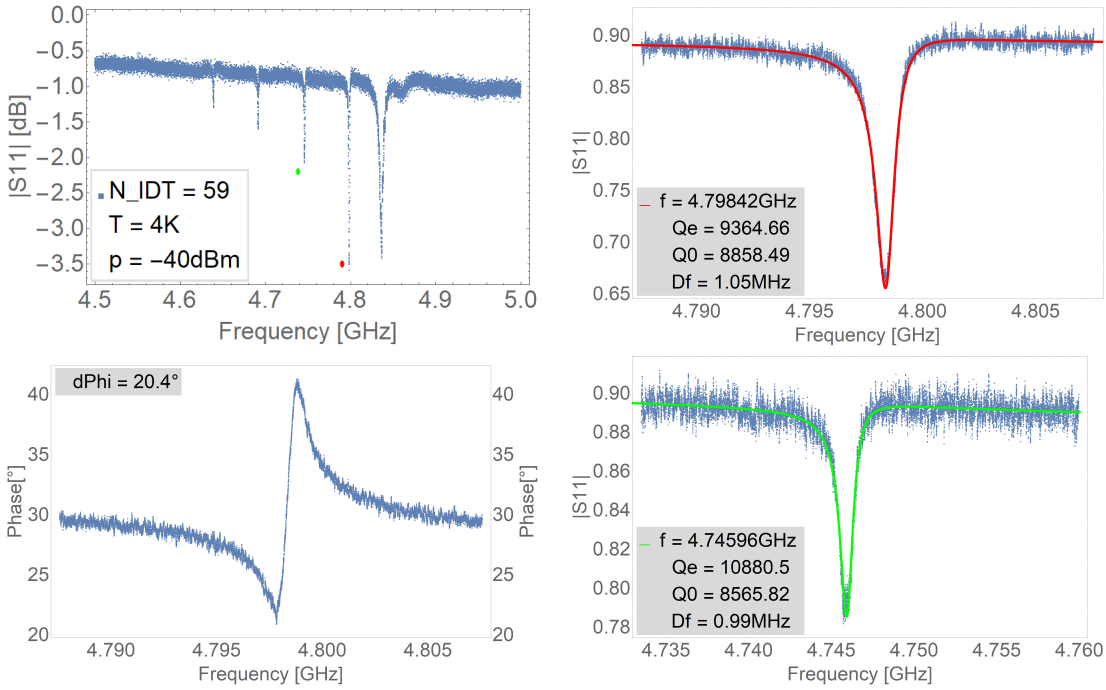

Figure 51: Number of fingers in the IDT = 39, 4K

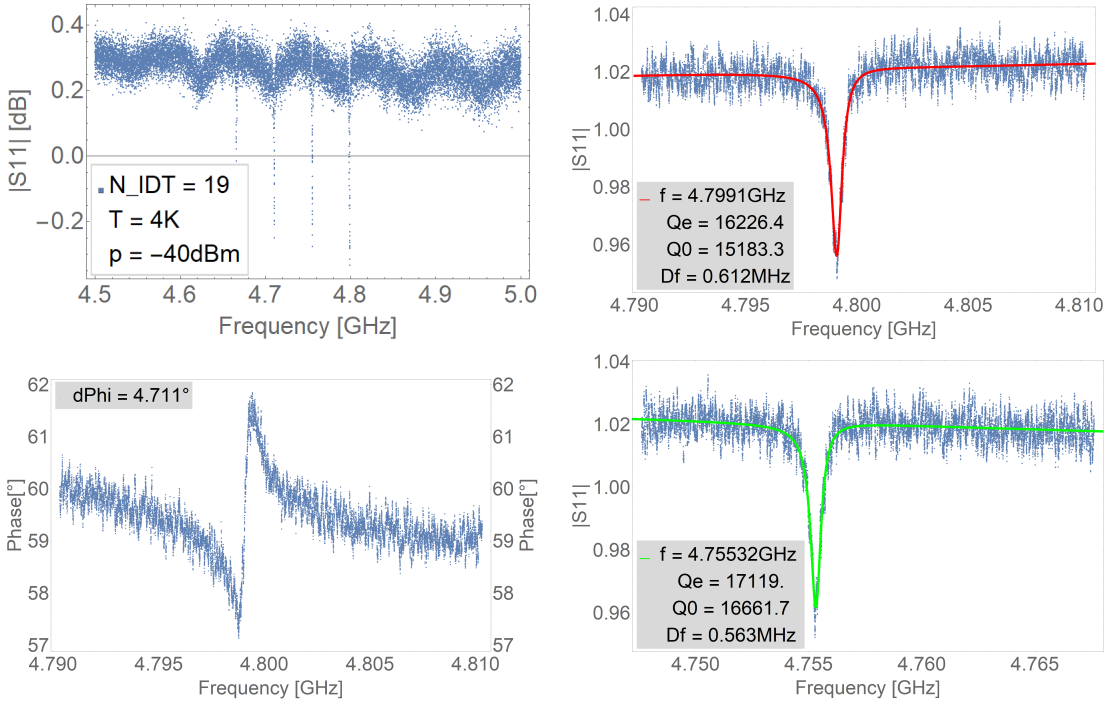

Figure 52: Number of fingers in the IDT = 19, 4K

4.5 Double Finger Transducers

As the previous results have shown that the mechanical reflections have a big impact on the quality factors of the SAW resonators, devices with IDT with double-fingers were fabricated. This design was tested on 4 resonators, which were pair-wise identical, the difference between the pairs being the SAW wavelength.

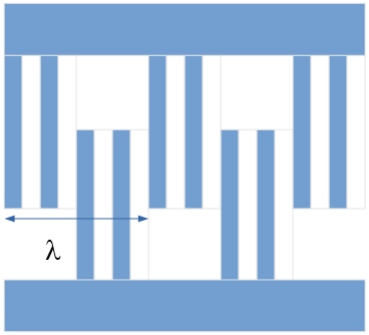

Figure 53: DDT Design: For the same wavelength, the features need to be half the size

Resonator	3 & 7	4 & 6
N_{IDT}	79 double pairs	
N_G	1000	
λ_0	700 nm	800 nm
d	201 λ_0	
W	100 λ_0	

Table 9: Properties of Sample

λ_0	Q_0 at RT	Q_{ext} at RT
700 nm	2022	22388
700 nm	4084	5390
800 nm	4062	6966
800 nm	3803	7874

Table 10: Quality factors for the two double finger devices at RT

As expected, the resonator spectrum is more symmetrical with respect to the SAW resonators with single-finger IDTs. This double finger device seems to be more suited for later implementations of SAW cavities coupled to artificial atoms, but further studies will have to be made to understand better the exact geometries that should be used to optimize this transducer design.

Resonator	Peak 1		Peak 2		Peak 3	
	Q_0	Q_{ext}	Q_0	Q_{ext}	Q_0	Q_{ext}
3	8509	10002	9282	10062		
7	13413	13473	12348	12775	13320	13947
4	11573	12495	11881	12208	11106	11357
6	11678	12317	12277	12334		

Table 11: Quality factors for the two double finger devices at 4K for different peaks

Room Temperature

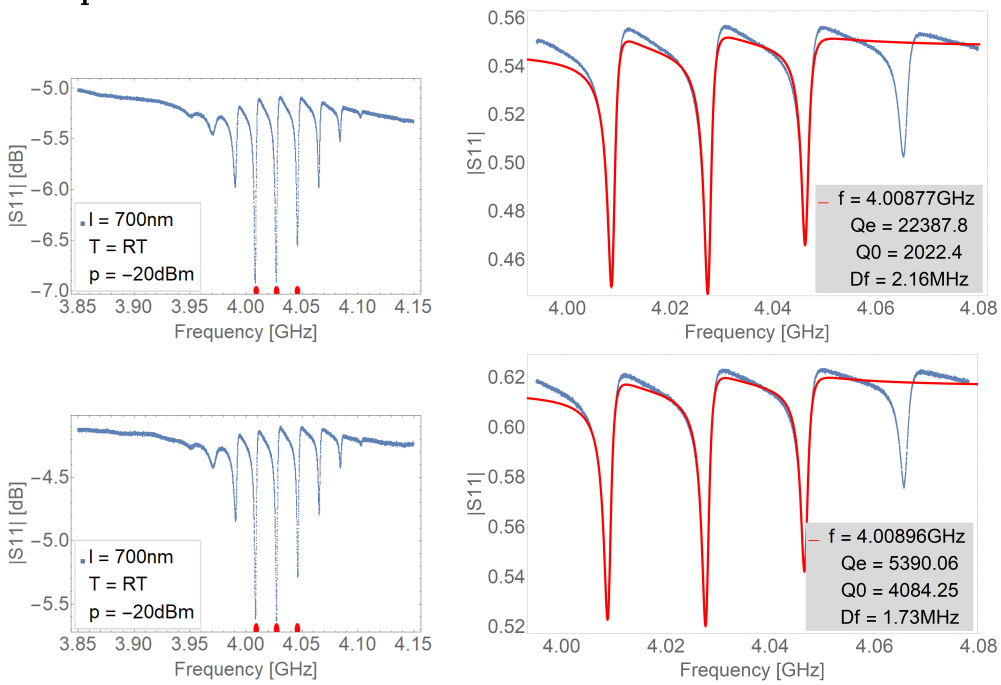

Figure 54: Resonators 3 (top) and 7 (bottom), 700nm, RT

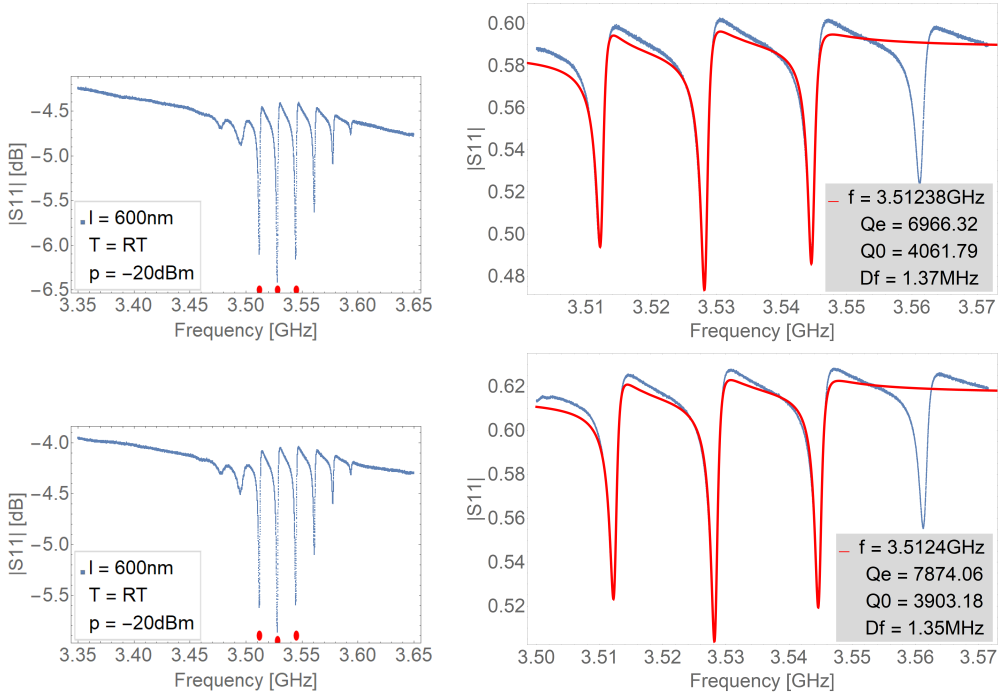

Figure 55: Resonators 4 (top) and 6 (bottom), 800nm, RT

4K

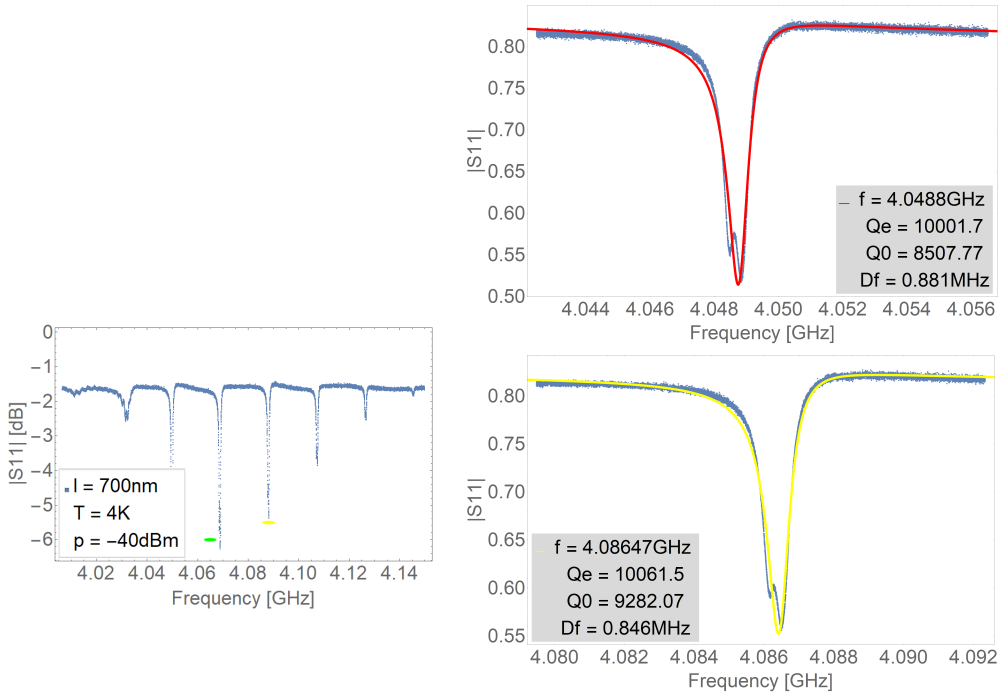

Figure 56: Resonator 3, 700nm, 4K

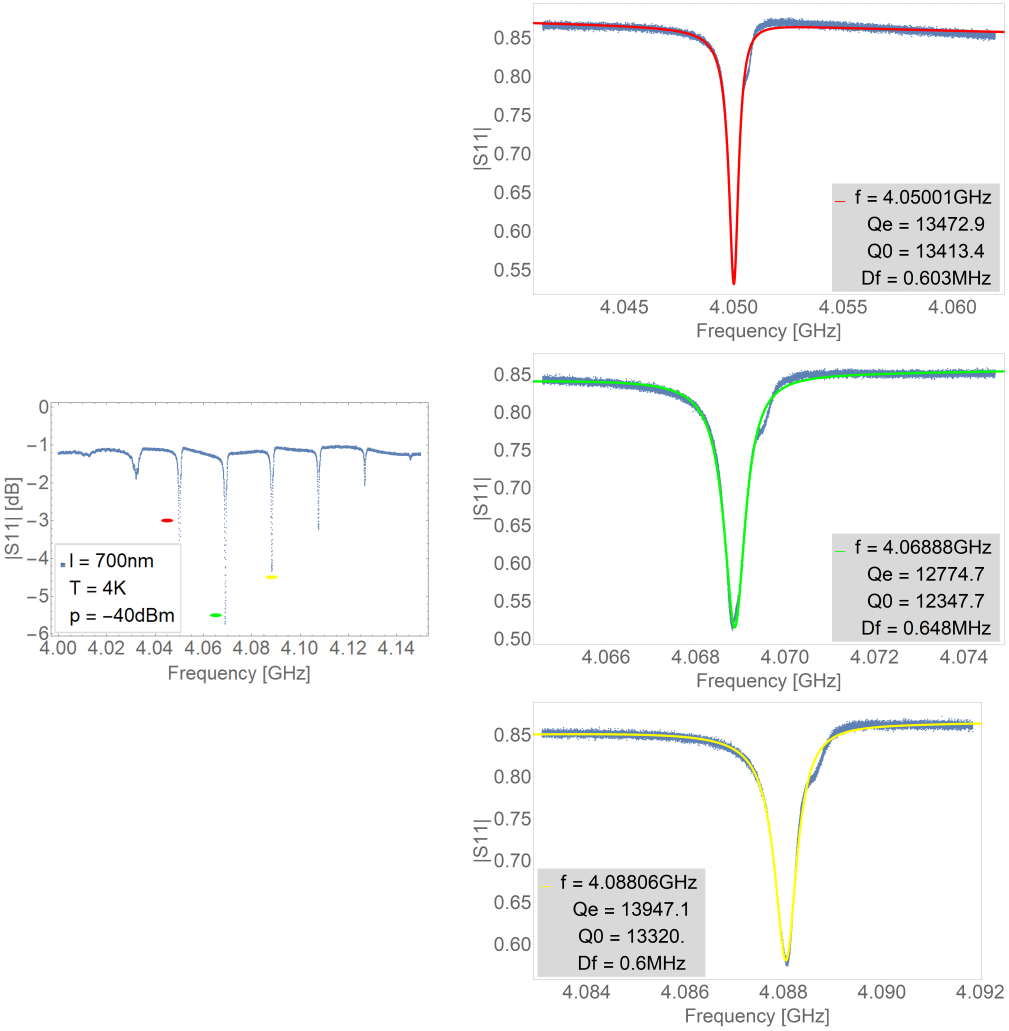

Figure 57: Resonator 7, 700nm, 4K

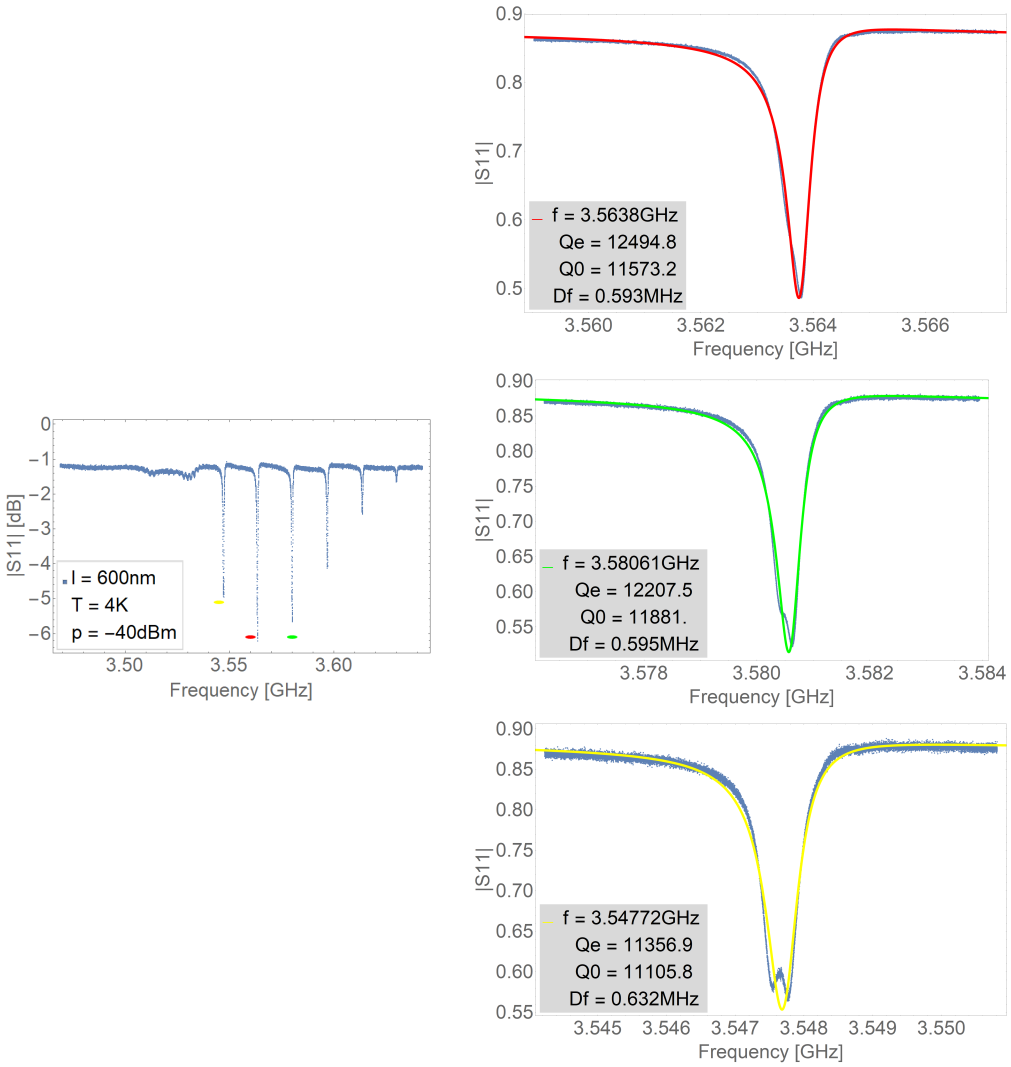

Figure 58: Resonator 4, 800nm, 4K

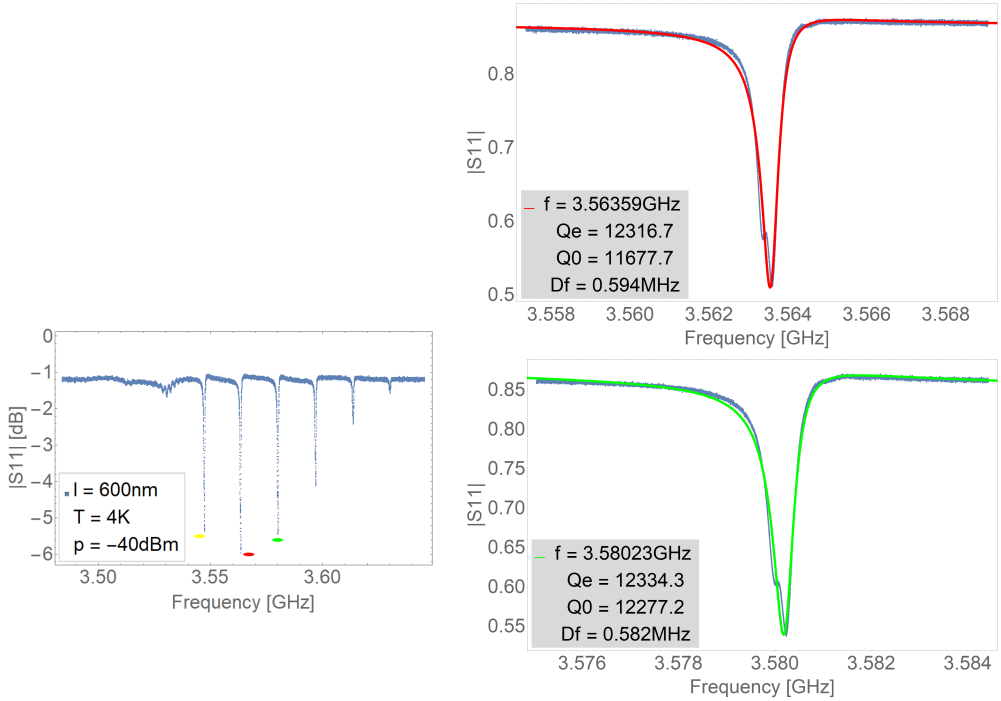

Figure 59: Resonator 6, 800nm, 4K

5 Conclusion

During this project, we analysed the dependence of the SAW resonator signal visibility and quality factors from many of the geometrical parameters defining the surface acoustic wave resonators. Many of these results showed that the influence of the mechanical reflections on the single finger IDT, considerably alters the SAW cavity spectrum, determining that the IDT acts also unexpectedly as a mirror. This results into the splitting of the designed SAW cavity into 2 sub cavities, partially decoupled by he IDT itself, drastically modifying the expected cavity spectrum. But the reflectivity of the Al fingers was determined on two different experimental series, making this result more trustful. The surface acoustic wave resonators investigated in this project are able to reach sub-MHz linewidths at 4K, which shows that they can be tentatively used in circuit quantum electrodynamic experiments [5].
To reduce the IDT mechanical reflections and have better control of the quality factors by fabrication, the double finger IDT design can be used, which mostly suppresses these unwanted effects.

6 References

[1] Thomas Aref, Per Delsing, Maria K. Ekstrom, Anton Frisk Kockum, Martin V. Gustafsson, Goran Johansson, Peter Leek, Einar Magnusson and Riccardo Manenti, *Quantum Acoustics with Surface Acoustic Waves*, Superconducting Devices in Quantum Optics (Springer, 2016), arXiv:1506.01631

[2] R. Manenti, M. J. Peterer, A. Nersisyan, E. B. Magnusson, A. Patterson and P. J. Leek, *Surface acoustic wave resonators in the quantum regime*, PRB **93**, 041411 (2016)

[3] M. J. A. Schuetz, E. M. Kessler, G. Giedke, L. M. K. Vandersypen, M. D. Lukin, J. I. Cirac, *Universal Quantum Transducers Based on Surface Acoustic Waves*, PRX **5**, 031031 (2015)

[4] J. Majer, J. M. Chow, J. M. Gambetta, Jens Koch, B. R. Johnson, J. A. Schreier, L. Frunzio, D. I. Schuster, A. A. Houck, A. Wallraff, A. Blais, M. H. Devoret, S. M. Girvin, R. J. Schoelkopf, *Coupling superconducting qubits via a cavity bus*, Nature **449**, 443 (2007)

[5] A. Wallraff et al., *Strong coupling of a single photon to a superconducting qubit using circuit quantum electrodynamics*, Nature **431**,162-167 (2004)

[6] Supriyo Datta, *Surface Acoustic Wave Devices*, Prentice Hall (1986)

[7] W. G. van der Wiel et al., *Electron transport through double quantum dots*, Rev. Mod. Phys. **75**, 1 (2002)

[8] A. J. Slobodnik Jr., *Attenuation of Microwave Acoustic Surface Waves Due to Gas Loading*, Journal of Applied Physics **43**,2565 (1972)

[9] David M. Pozar, *Microwave Engineering*, Wiley (2011)

[10] Riccardo Manenti, *Surface Acoustic Wave Resonators for Quantum Information*, Master's Thesis, Leek Lab, University of Oxford

Eidgenössische Technische Hochschule Zürich
Swiss Federal Institute of Technology Zurich

Declaration of originality

The signed declaration of originality is a component of every semester paper, Bachelor's thesis, Master's thesis and any other degree paper undertaken during the course of studies, including the respective electronic versions.

Lecturers may also require a declaration of originality for other written papers compiled for their courses.

I hereby confirm that I am the sole author of the written work here enclosed and that I have compiled it in my own words. Parts excepted are corrections of form and content by the supervisor.

Title of work (in block letters):

Surface Acoustic Wave Resonators

Authored by (in block letters):

For papers written by groups the names of all authors are required.

Name(s):	**First name(s):**
Loos	Denis

With my signature I confirm that

- I have committed none of the forms of plagiarism described in the 'Citation etiquette' information sheet.
- I have documented all methods, data and processes truthfully.
- I have not manipulated any data.
- I have mentioned all persons who were significant facilitators of the work.

I am aware that the work may be screened electronically for plagiarism.

Place, date	**Signature(s)**
Zurich, 28/11/2017	Denis Loos

For papers written by groups the names of all authors are required. Their signatures collectively guarantee the entire content of the written paper.